AD_____

Award Number: W81XWH-04-1-0222

TITLE: Analysis of Morphogenic Effect of hDAB2IP on Prostate Cancer and its Disease Correlation

PRINCIPAL INVESTIGATOR: Jer-Tsong Hsieh, Ph.D.

CONTRACTING ORGANIZATION: University of Texas, Southwestern Medical Center
Dallas, TX 75390-9110

REPORT DATE: February 2006

TYPE OF REPORT: Annual

PREPARED FOR: U.S. Army Medical Research and Materiel Command
Fort Detrick, Maryland 21702-5012

REPORT DOCUMENTATION PAGE

Form Approved
OMB No. 0704-0188

1. REPORT DATE *(DD-MM-YYYY)*	**2. REPORT TYPE**	**3. DATES COVERED** *(From - To)*
01-02-2006	Annual	1 Feb 2005 - 31 Jan 2006

4. TITLE AND SUBTITLE
Analysis of Morphogenic Effect of hDAB2IP on Prostate Cancer and its Disease Correlation

5a. CONTRACT NUMBER

5b. GRANT NUMBER
W81XWH-04-1-0222

5c. PROGRAM ELEMENT NUMBER

6. AUTHOR(S)
Jer-Tsong Hsieh, Ph.D.

E-Mail: JT.Hsieh@UTSouthwestern.edu

5d. PROJECT NUMBER

5e. TASK NUMBER

5f. WORK UNIT NUMBER

7. PERFORMING ORGANIZATION NAME(S) AND ADDRESS(ES)
University of Texas, Southwestern Medical Center
Dallas, TX 75390-9110

8. PERFORMING ORGANIZATION REPORT NUMBER

9. SPONSORING / MONITORING AGENCY NAME(S) AND ADDRESS(ES)
U.S. Army Medical Research and Materiel Command
Fort Detrick, Maryland 21702-5012

10. SPONSOR/MONITOR'S ACRONYM(S)

11. SPONSOR/MONITOR'S REPORT NUMBER(S)

12. DISTRIBUTION / AVAILABILITY STATEMENT
Approved for Public Release; Distribution Unlimited

13. SUPPLEMENTARY NOTES

14. ABSTRACT:

Prostate homeostasis is a balance between cell proliferation, apoptosis and differentiation in basal and luminal epithelia. It is believed that loss of homeostatic control in these cells renders the onset of neoplasm in prostatic epithelium. Until now, a little is known about homeostatic machinery in normal prostatic epithelium. In this project, we have proposed that DAB2IP protein, a novel RASGAP, is a part of homeostatic machinery and plays an important in modulating signal pathways elicited by exogenous growth/death stimuli. For example, DAB2IP is able to counteract androgen-mediated cell growth and is involved in TNF-α-mediated cell apoptosis. We further demonstrated that decreased steady-state levels of DAB2IP in normal prostatic epithelium resulted in the tumor formation of these cells. Further investigation has led us to unveil the underlying mechanism of DAB2IP in modulating specific signal cascades.

15. SUBJECT TERMS
Cell differentiation, GTPase activating protein, tumor suppressor, Epigenetic regulation, signal transduction, prostate cancer

16. SECURITY CLASSIFICATION OF:			**17. LIMITATION OF ABSTRACT**	**18. NUMBER OF PAGES**	**19a. NAME OF RESPONSIBLE PERSON**
a. REPORT	**b. ABSTRACT**	**c. THIS PAGE**			USAMRMC
U	U	U	UU	52	**19b. TELEPHONE NUMBER** *(include area code)*

Table of Contents

INTRODUCTION

In prostate cancer (PCa), enhanced expression of RAS protein correlates with increased tumor grade (1). Expression of RAS protein has also been assessed in primary and metastatic tumors. Results (1-3) indicated that most metastatic tumors expressed RAS protein, while only a fifth of primary tumor did. Data from clinical specimens and animal models demonstrate that the increased c-H-RAS mRNA expression in PCa reflects the progression of PCa from AD to AI. Surprisingly, PCa cells demonstrate an extremely low rate of mutation in the RAS gene (3, 4). This implies that other effectors regulating RAS activity may be involved in increasing RAS protein levels in PCa.

We identified DAB2IP as a new member of GAP family as a potent growth inhibitor in AIPCa cell lines and the down regulation of DAB2IP is often associated with many androgen-independent PCa cell lines. The amino acid sequence homology between DAB2IP and the GAP domain of other RASGAPs suggests that DAB2IP may have the GTPase activity of RAS. Our *in vitro* and *in vivo* results demonstrate that DAB2IP stimulates GTPase activity of RAS in a dose dependent manner and its GAP activity was similar with $p120^{GAP}$, indicating that DAB2IP is a typical RASGAP. Unlike classical $p120^{GAP}$, DAB2IP contains several other functional motifs such as Pleckstrin Homology (PH) domain (aa 20-70) with a high affinity to specific phosphoinositides, C2 domain (aa 90-120) involved in binding phospholipids in a calcium dependent manner or calcium independent manner, proline-rich (PR) domain (aa 725-734) involved in interacting with proteins containing SH3 domain (5), and a leucine zipper (aa 840-859), which is a protein-protein dimerization domain (6). For example, we have shown that the C2 domain of DAB2IP is involved in the TNF-α-mediated apoptosis by activating apoptosis-stimulated kinase (7). Thus, DAB2IP in addition to its GAP activity should have multiple functional roles in controlling the physiology of cell.

RECENT PROGRESS

We are the first group to report that DAB2IP is an Ezh2 target gene in PCa, which underlies the mechanism of elevated Ezh2 in PCa cells; this work has been published in Journal of Biologic Chemistry and the other manuscript has been accepted for publication (Appendix 1-2). The third manuscript is in preparation for describing the status of DAB2IP gene methylation in clinical specimens. Overall, Task 1 is completed; Task 2 is 70% completed and Task 3 is underway with very good progress. In summary, we made several key progresses in this project: (1) to examine the effect of DAB2IP on androgen-elicited cell growth and -regulated genes; (2) to determine the tumor growth of normal prostatic epithelium with decreased endogenous DAB2IP expression; (3) to unveil the promoter and its regulation of mouse DAB2IP gene; (4) to demonstrate the involvement of DAB2IP in TNF-α-elicited apoptosis of PCa via the interaction of apoptosis-signal-regulated kinase1 (ASK1). Thus, I have summarized these new results as follows:

Task 2. To study the function role of hDAB2IP protein complex in prostatic epithelial differentiation.

A. <u>The inhibitory effect of DAB2IP on androgen-elicited cell growth of prostate cancer</u>

Using DAB2IP stable transfectant (D1) (8) and its parental C4-2 cells, data from Figure 1 indicated that the presence of DAB2IP was able to intervene androgen-elicited cell growth.

Consistently, androgen was able to induce Erk activation in C4-2 cells in a dose-dependent manner, however, no increase in Erk activation is detected in D1 cells. Based on data from microarray (GEArray Q series, SuperArray Bioscience Corporation) containing 96 known AR-regulated genes validated qRT-PCR (Figure S2), we believe that DOC-2/DAB2 does not influence the expression of AR-regulated genes. Taken together, these data indicate that DAB2IP can block AR-mediated cell growth via non-genomic pathway (i.e., protein interaction or post-translation modification).

Figure 1 Inhibitory effect of DAB2IP on androgen-induced cell proliferation of PCa. A, Cells were incubated with various amounts of DHT for 4days, and the cell proliferation was determined by MTT assay. B, The inactivation of Erk2 phosphorylation (pErk) in D1 cells. Erk, total Erk as the internal control.

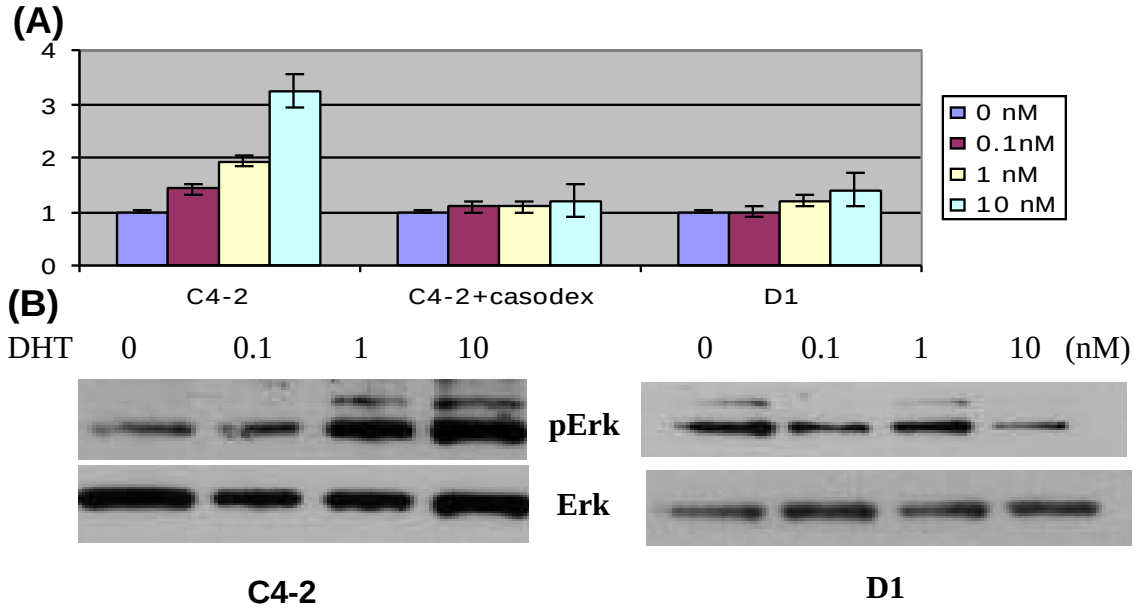

Figure 2 Validation of androgen-regulated genes using real-time RT-PCR. The cDNA was synthesized from the same RNA source used for array screening and subjected to real-time RT-PCR for several potential candidate genes.

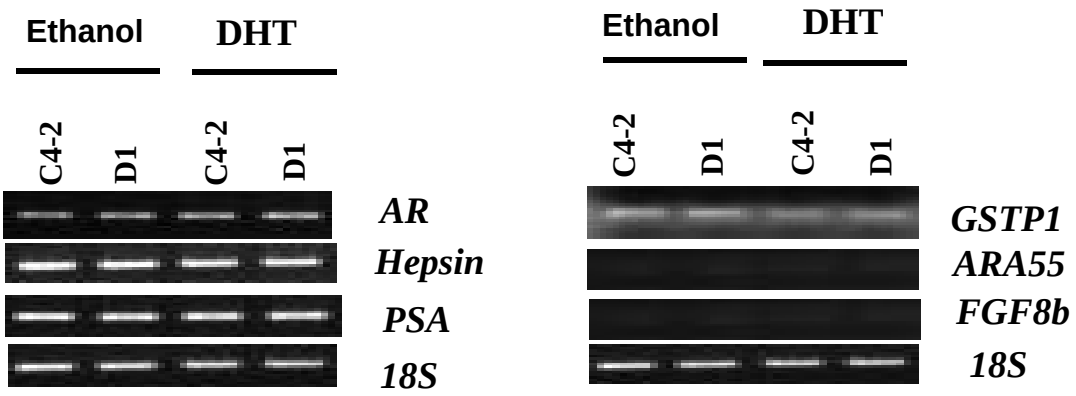

B. <u>Increased tumor growth of prostatic epithelia with decreased endogenous DAB2IP gene</u>

On the other hand, we examined whether non-tumorigenic prostatic epithelial cell (PZ-HPV-7) could become tumorigenic once the endogenous DAB2IP levels were down regulated. Data from Figure 2A indicated that the endogenous DAB2IP levels were knock down in two sublines (i.e., CL1 and CL2) of PZ-HPV-2 cells transfected with DAB2IP SiRNA expression vector compared with parental or vector control cells. By injecting these cells into athymic nude mouse, we were able to observe increased tumor take (CL1: 6/10; CL2 8/10) and growth of PZ-HPV-2 sublines (Figure 2B). Currently, we are implanting these cells into subrenal capsule to observe any morphologic alteration. These data clearly indicate that DAB2IP is a potent tumor suppressor in PCa development.

Figure 2 Increased tumorigenicity of PZ-HPV-7 by reducing endogenous DAB2IP expression. A, Total cell lysate of different clones of transfectant was subjected to western blot analysis. B, An equal number ($1X10^6$ /site) of cells was injected subcutaneously into 5 athymic mice per group (2 sites/animal). Tumor volume was determined weekly by caliper (9). P: Parental; C: vector control; CL1: Clone 1; CL2, Clone 2

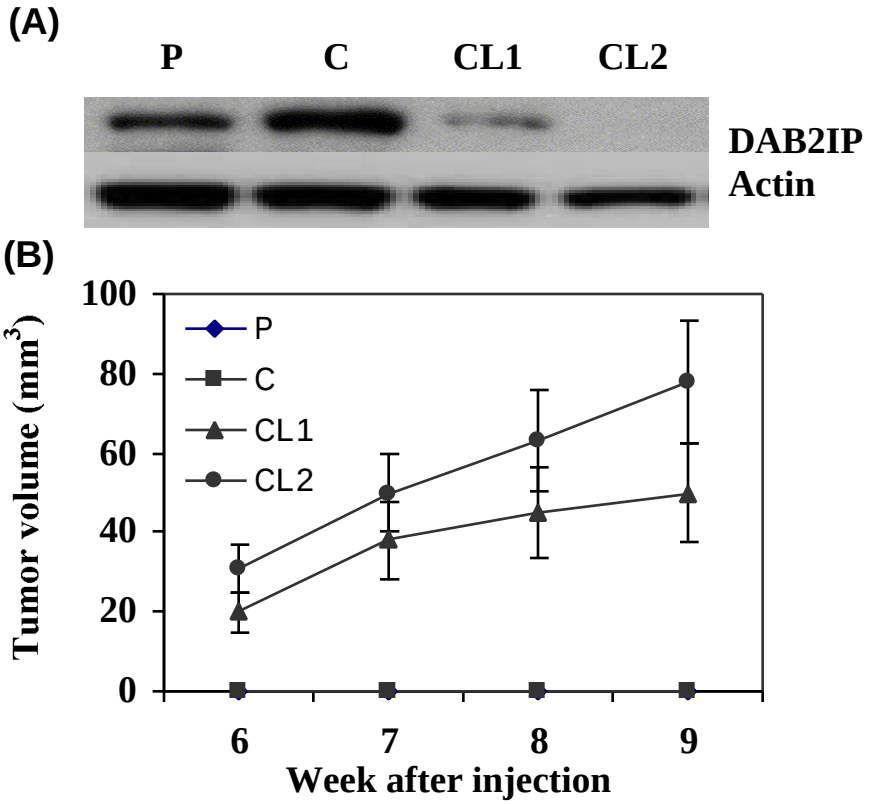

B. <u>Characterization of mouse DAB2IP gene promoter and its promoter</u>

We are planning to generate DAB21P knock out mouse. Thus, we isolated the mouse Dab2iP gene with a highly homologous sequence to that of the human and rat gene and mapped it at chromosome 2B (see Appendix 1). Overall, the mDAB2IP gene contains 14 exons and 13 introns and spans approximately 65kb. Exon1 contains at least three variants, exon Ia; exon Ib and exon Ic. Data from real-time RT-PCR analysis revealed a diverse expression pattern of *mDab2ip* gene in various organs, implying that differential regulation of this gene from various tissues. We have mapped a 1.3kb segment containing 5'-upstream region from exon Ia as a

promoter region (–147/+545) in prostatic epithelial cell lines (TRAMP-C); this region is highly GC-rich and *mDab2ip* appears to be a TATA-less promoter. Unlike human PCa cell, DAB2IP gene promoter is regulated by histone acetylation but slight effect DNA methylation in mouse PCa cell (see Appendix 2).

Task 3. To delineate signal cascade mediated by hDAB2IP protein complex in prostatic epithelium.

B. **The role of DAB2IP in TNF-α-induced cell death**

TNF-α is known as a potent agent in inducing cell apoptosis in C4-2 (Table 1). Since DAB2IP is able to interact with ASK1 in endothelial cell (7), we have further investigated the possible involvement of DAB2IP in TNF-α-mediated signal pathway could be involved in TNF-α-induced cell death in PCa. To demonstrate the involvement of ASK1 in this process, we performed co-immunoprecipitation assay to examine this possibility. Data (Figure 3) indicated that TNF-α only induced DAB2IP expression in C4-2 as shown previously. For the endogenous ASK1 protein levels in C4-2 cells, TNF-α did not alter its expression. Noticeably, the interaction between DAB2IP and ASK1 was significantly enhanced by TNF-α. These data suggest that ASK1 should be involved in TNF-α-induced cell death in PCa. Currently, we are working to knock down the endogenous ASK1 or DAB2IP in C4-2 and determine the effect of TNF-α in terms of cell death induction.

Table 1 Cell cycle analyses of C4-2 cells treated with different concentrations of TNF-α

	2 days				3 days			
ng/ml	0	0.1	1	10	0	0.1	1	10
Sub-G_1	7.3	8.9	9.5	18.3	6.3	7. 1	27.7	49.4
G_1/G_0	44.9	43.6	62.6	62.1	40.9	45.8	53.6	34.1
S phase	30.8	31.5	17.4	10.3	35.8	29.8	10.0	8.2
G_2/M	17.0	16.0	10.5	9.3	17.0	17.3	8.7	8.3

Each number was averaged from three different measurements from cytometrical analyses and variation is less than 10%.

Figure 3 The interaction between DAB2IP and ASK1 in TNF-α-treated C4-2 cells. Cells were treated with different concentration of TNF-α (0, 1, 10 ng/ml) for 24 hrs, total cell lysate was prepared and subjected to western blot analysis (A) or immunoprecipitation with DAB2IP antibody then probed with ASK1 antibody (B).

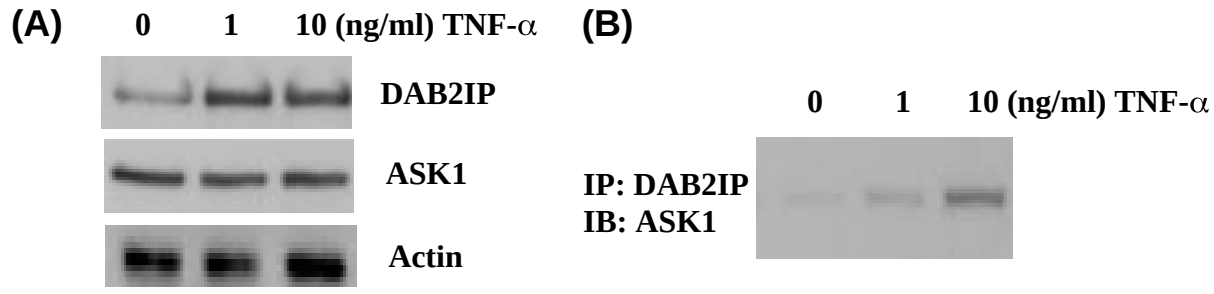

KEY RESEARCH ACCOMPLISHMENT

- Determine the effect of DAB2IP on androgen-elicited cell growth in PCa.
- Identify the mechanism of action of DAB2IP in suppressing non-genomic pathway of androgen in PCa.
- Generate a DAB2IP SiRNA expression vector.
- Knock down endogenous DAB2IP gene expression in prostatic epithelium and characterize its biologic behavior.
- Clone and characterize mouse DAB2IP gene and its promoter.
- Profile the DAB2IP gene expression in various mouse organs and PCa cells.
- Determine the epigenetic regulation of mouse DAB2IP gene in muse PCa cells.
- Determine the possible role of DAB2IP in TNF-α-elicited cell apoptosis of PCa cells.
- Demonstrate the interaction between ASK1 and DAB2IP in PCa cells induced by TNF-α.

REPORTABLE OUTCOMES

FULL-LENGTH PAPER

1. Chen, H, and Hsieh, J.T. (2005) Down regulation of human DAB2IP gene expression mediated by polycomb Ezh2 complex and histone deacetylase in prostate cancer. J. Biol. Chem., 280: 22437-22444.

2. Chen, H, Karam. J.A., Schultz, R., Zhang, Z., Ducan, C., and Hsieh, J.T. (2006) Cloning of *mDAB2IP* gene, a novel member of the RasGTPase-activating protein family and characterization of its regulatory region. Cytogenetics and Genome Res., (In press)

REVIEW PAPER

1. Karam J., Benaim, E., Chen, H., Pong, R.C., and Hsieh, J.T. (2005) Epigenetics in prostate cancer. In Prostate Cancer: Mechanisms, Prevention, and Hormone Therapy (Chang, C., ed) World Scientific, pp 213-228.

CONCLUSIONS

Prostate homeostasis relies on a balance between cell proliferation, apoptosis and differentiation. Androgens, and more specifically dihydrotestosterone (DHT), are essential but are not directly responsible for prostatic growth as it has been supported by observations such as cultured normal epithelial cells isolated from basal cell do not respond to androgen and prostate stromal cells with androgen receptor (AR) under androgen stimulation produce andromedin (10) that is a potent mitogen for prostate epithelia. On the other hand, androgen also appears to be a morphogen because androgen is required for architect, secretory function and survival of luminal cell, indicating that androgen can orchestrate the effects of growth stimulatory and differentiation factors via paracrine and/or autocrine manner. Indeed, cross talks between different signaling axes are increasingly regarded as fundamentally important to the development, growth and maintenance of homeostasis in the prostate. In contrast, androgen becomes a potent mitogen for PCa, indicating the normal physiologic function of androgen is impaired in the malignant cells. Based on our study, DAB2IP appears to be a part of homeostatic machinery to modulate normal growth and differentiation of prostatic epithelium. Consistently, loss of DAB2Ip is often detected in PCa. Further study of the role of DAB2IP in signal transduction will provide more understanding of homeostatic control of prostatic epithelium.

REFERENCES

1. Viola, M. *et al.* (1986) Expression of ras oncogene p21 in prostate cancer. N. Eng. J. Med., 314: 133-137.
2. Sumiya, H. *et al.* (1990) Histochemical examination of the expression of ras p21 protein and R-1881-binding protein in human prostatic cancer. Eur J. Cancer, 26: 786-789.
3. Carter, B.S., Epstein, J.I., Isaacs, W.B. (1990) ras gene mutation in human prostate cancer. Cancer Res., 50: 6830-6832.
4. Gumerlock, P.H. *et al.* (1991) Activated ras alleles in human carcinoma of the prostate are rare. Cancer Res., 51: 1632-1637.
5. Scheffzek, K. *et al.* (1997) The Ras-RasGAP complex: structural basis for GTPase activation and its loss in oncogenic Ras mutants. Science, 277: 333-338.
6. Struhl, K. (1989) Helix-turn-helix, zinc-finger, and leucine-zipper motifs for eukaryotic transcriptional regulatory proteins. Trends in Bioch. Sci., 14: 137-140.
7. Zhang, R. *et al.* (2003) AIP1 mediated TNF-induced ASK1 activation by facilitating dissociation of ASK1 from inhibitor 14-3-3. J. Clin. Invest., 11, 1933-1943.
8. Wang, Z. *et al.* (2002) A Novel RasGTPase activating protein that interacts with DOC-2/DAB2: A downstream effector leading to the suppression of prostate cancer. J. Biol. Chem., 277, 12622-12631.
9. Okegawa, T. *et al.* (2005) Enhanced transgene expression in urothelial cancer gene therapy with histone deacetylase inhibitor. J. Urol., 174: 747-752.
10. Lu, W. *et al.* (1999) Fibroblast growth factor-10.: Asecond candidate stromal to epithelial cell andromedin in prostate. J. Biol. Chem., 274: 12827-12834.

To: JT Hsieh
From: Jennifer Wolfe <wolfe@reo.med.upenn.edu>
Subject: Manuscript submitted to "DNA & Cell Biology"
CC:
Date Sent: Wednesday, January 18, 2006 10:29 AM

Dear Dr. Hsieh:

Thank you for submitting the manuscript, "Cloning of mouse Dap2ip gene, a novel member of the RasGTPase-activating protein family and characterization of its regulatory region in prostate" which has now been accepted for publication in DNA and Cell Biology.

Please send a CD of your manuscript as soon as possible so that the publishers can access it electronically. When that is received, the manuscript will be sent off to the publishers for typesetting and they will contact you regarding the page-proofs. Thank you.

Sincerely,

Mark I. Greene

--
Jennifer Wolfe
Assistant to Mark I. Greene, M.D., Ph.D., F.R.C.P.
University of Pennsylvania School of Medicine
Department of Pathology and Laboratory Medicine
252 John Morgan Building
36th Street and Hamilton Walk
Philadelphia, PA 19104-6082
Phone: 215-898-2868
Fax: 215-898-2401
email: wolfe@reo.med.upenn.edu

Cloning of mouse *Dab2ip* gene, a novel member of the RasGTPase-activating protein family and characterization of its regulatory region

Hong Chen[1], Jose A Karam[1], Roger Schultz[2], Zhengwang Zhang[1], Christine Duncan[2] and Jer-Tsong Hsieh[1]

Department of Urology[1] and Pathology[2], University of Texas Southwestern Medical Center, Dallas, TX 75390-9110 (USA)

* Address all correspondence to:
J.T. Hsieh, Ph.D.
University of Texas Southwestern Medical Center
Department of Urology
5323 Harry Hines Blvd.
Dallas, TX 75390-9110
(Phone) 214-648-3988
(Fax) 214-648-8786
(E-mail) JT.Hsieh@UTSouthwestern.edu

Sequence data from this article have been deposited into the EMBL/GenBank Data Libraries under accession number AY305656, AY305657 andAY305658

Key words: ***Dab2ip* gene, prostate cancer, gene promoter**

ABSTRACT

Disabled homolog 2 (Drosophila) interacting protein (DAB2IP/Dab2IP) is a member of GTPase-activating protein for down-regulating the Ras-mediated signal pathway and TNF-mediated apoptosis. The down regulation of human *DAB2IP* mRNA levels was detected in prostate cancer cells due to the epigenetic regulation. Here, we isolated a mouse *Dab2ip* gene with a highly homologous sequence to that of the human and rat gene and mapped it at chromosome 2B. The *mDab2ip* gene contains 14 exons and 13 introns and spans approximately 65kb. Exon1 contains at least three splicing variants (Ia, Ib, and Ic). The deduced amino acid sequence of mouse Dab2IP encompasses 1,065 residues containing several unique protein interaction motifs as well as a Ras-like GAP-related domain, which shares a high homology with both human and rat. Data from real-time RT-PCR analysis revealed a diverse expression pattern of *mDab2ip* gene in various organs, implying that differential regulation of this gene from various tissues. We have mapped a 1.3kb segment containing 5'-upstream region from exon Ia as a promoter region (–147/+545) in prostatic epithelial cell lines (TRAMP-C); this region is highly GC-rich and *mDab2ip* appears to be a TATA-less promoter. Unlike human prostate cancer cell, *Dab2ip* gene promoter is regulated by histone acetylation but slight effect DNA methylation in mouse prostate cancer cell.

INTRODUCTION

Disabled homolog 2 (Drosophila) interacting protein (DAB2IP/Dab2IP) is a novel member of the Ras GTPase-activity family protein (Chen *et al.,* 2002; Wang *et al.,* 2002) DAB2IP is able to interact with DOC-2/DAB2 (Zhou and Hsieh, 2001; Fulop *et al.,* 1998; Tseng *et al*., 1999; Zhou *et al*., 2003) and this protein complex modulates Ras-mediated signal pathway then causes the growth inhibition in prostate cancer cells (Wang *et al*., 2002). Also, DAB2IP (also named AIP1: ASK interacting protein 1) is involved in TNF-α-mediated cell apoptosis by facilitating dissociation of ASK1 from its inhibitor 14-3-3 (Zhang *et al*., 2003, Zhang *et al.,* 2004)

The higher *hDAB2IP* mRNA levels are detected in normal human prostatic epithelium than in prostate cancer cells, which is due to the epigenetic regulation (Jones *et al.,* 2001; Wolffe and Matzke, 1999) such as DNA methylation and histone acetylation of human *DAB2IP* (*hDAB2IP)* gene promoter (Chen *et al*., 2002, 2003). In breast cancer, DNA hypermethylation of *hDAB2IP* is also found in both breast cancer cell lines and specimens with lymph node metastasis, and *hDAB2IP* gene expression can be restored in methylated cell lines treated with 5-aza-2´-deoxycytidine (Dote *et al.,* 2004). Also, *hDAB2IP* (alias for AFQ34) is identified as a novel MLL fusion partner from an acute myeloid leukemia patient with a t(9;11)(q34;q23); the intron 9 of MLL gene is translocated into the exon 2 of *DAB2IP* and causes the disruption of pleckstrin homology (PH) domain in DAB2IP protein, implying that this fusion protein may alter RAS activity as a part of leukemia transformation process (von Bergh *et al*., 2004). Thus, DAB2IP should be involved in carcinogenesis of various tissues.

To further unveil the physiological functions of mouse *Dab2ip*, we decided to clone and map its chromosomal location. With analyzing the structure of mouse *Dab2ip* (*mDab2ip*) gene, we have assembled the entire gene sequence and its full-length mRNA with an open reading frame. We also profiled the *mDab2ip* expression pattern from a variety of organs and cell lines. By determining the promoter sequence from the 5'-flanking region of the *m Dab2ip* gene in mouse prostatic epithelial cell lines provided clues for the transcriptional regulation of *mDab2ip* gene.

MATERIALS AND METHODS

Tissue Culture, Treatment and RNA isolation

Three mouse transgenic prostate adenocarcinoma cell lines (TRAMP-C1, TRAMP-C2 and TRAMP-C3*)* (Foster *et al*., 1997; Greenberg *et al*., 1995; Gingrich *et al.*, 1997) were maintained in DMEM supplemented with 5% FBS (HyClone, Logan, UT) plus 5% Nu-serum^{TM} IV (BD Bioscience, Bedford, MA) and 50ng/ml insulin (Sigma). NIH-3T3 cell line was maintained in DMEM with 10% FBS and PC3 cell line was maintained in T medium supplemented with 5% FBS. Total RNA from variant organs and cell lines were isolated using the RNAzol B (Tel-Test Inc., Friendswood, TX) according to the manufacturer's instructions.

For tissue RNA isolation, various organs (approximate 50 mg) were harvested from nude mice after euthanasia and were snap-frozen in liquid nitrogen until analysis was performed. Tissues were submerged with RNAzol B and quickly homogenized then subjected to the same isolation procedure.

To study the effect of hisone acteylation, different concentrations (20, 40, 100 nM) of Trichostatin (TSA) was changed every 24 hrs for 48 hrs. For studying the effect of DNA methylation, different concentrations (1, 2, 5μM) of 5-aza-2´-deoxycytidine (5'-Aza) was changed every 48 hrs for 96 hrs. For the combination, TSA was added at 24 hrs and changed at 72 hrs, and 5'-Aza was replaced at 48 hrs. Cells were collected at 96 hrs after treatment.

Cloning mouse Dab2ip gene and sequence Analysis

To obtain the entire coding region of mouse *Dab2ip* cDNA, we performed RT-PCR from total cellular RNA from mouse brain. Based on the high homology sequences between human and rat *DAB2IP* cDNA (Chen *et al*., 2002; Wang *et al.,* 2002), two sets of primer were synthesized (Table 1). PCR products were cloned into pCR2.1-TOPO vector (Invitrogen) and sequenced, then used as probes for screening *mDab2ip* gene.

A mouse bacterial artificial chromosomal (BAC, RPCI.22) library (ResGen Invitrogen Corp. Huntsville, AL) was screened. The positive clones were subjected to Southern blot analysis and DNA sequencing for confirmation.

Identification of transcriptional starting site (TSS) by 5' RACE

To determine the transcriptional starting site of *mDab2ip* gene, The total cellular RNA (10 μg) from two mouse organs (brain and kidney) and two TRAMP-C lines (TRAMP-C1 and TRAMP-C2) was subjected to 5' RACE using the FirstChoice™ RLM-RACE Kit (Ambion Inc, Austin, TX) according to the manufacturer's manual. A random-primed reverse transcription reaction and nested PCR (Fig 2B and Table1) were performed to amplify the 5'end of the *mDab2ip* mRNA transcript. We analyzed the PCR product in a 2% NuSieveâ 3:1 agarose gel (Cambrex BioScience, Rockland, MA) and then cloned it into pCR2.1-TOPO for sequence identification.

Determination of mDAB2IP mRNA levels by Real-time quantitative RT-PCR (qRT-PCR) assay

Two micrograms of total cellular RNA were reversely transcribed into cDNA and amplified using either *mDab2ip* primer set (2 ng/μl) or *Actin* primer set (6 ng/μl) (Table 1) in a 40-μl reaction mixture containing 20-μl IQ^{TM} SYBR® Green Supermix (Bio-Rad Laboratories, Hercles). The PCR was performed using iCycler machine (Bio-Rad) and the reaction condition was as follow: 95°C (3 min) and 40 cycles amplification cycle (95°C [30 sec], 55°C [30 sec], and 72°C [1 min]). To assure the quality of each reaction, melting curves analysis was performed using 95°C (1 min), 55°C (1 min) and 80 cycles of 0.5°C increment beginning at 55°C. Each sample was performed in duplicates. The level of *m Dab2ip* mRNA from each organ was calculated as follows: ΔC_t (threshold cycle) of each sample = mean of $C_{t(Dab2ip)}$ - mean of $C_{t(Actin)}$. The relative expression of *m Dab2ip* in each organ was calculated as $1/2^{\Delta C_{t(\text{sample tissue})} - \Delta C_{t(\text{spleen})}}$ since spleen had the lowest *Dab2ip* mRNA level. Meanwhile, The levels of *mDab2ip* mRNA from each cell lines were calculated as $1/2^{\Delta C_{t(\text{sample cell})} - \Delta C_{t(\text{TRAMP-C3})}}$ since TRAMP-C3 had the lowest expression of *mDab2ip*.

Fluorescence in Situ Hybridization (FISH) analysis

To determine the chromosomal localization of the *mDab2ip* gene, cells were sterilely isolated from the spleens of 6-week old mice and set up in RPMI 1640 with glutamine, 20% FBS, and 50μg lipopolysaccharide at 37°C for 42 hours. At 42 hours 0.75μl of 10μg/ml colcemid was added and incubated for 10 minutes. Cells were pelletted, resuspended in 1 ml of hypotonic KCl (pre-warmed to 37°C) and incubated at

room temperature for 15 minutes. The cells were then fixed in methanol**:** acetic acid (3**:**1) and spread on slides using heat treatment. DNA probes from BAC clones 22N15 and 301E21 were fluorescently labeled by nick translation using standard conditions. Probe was hybridized to mouse metaphase slides overnight on a HYBrite (Vysis, Inc., Downers Grove, IL) hybridization chamber and washed. Hybridization signal was viewed and analyzed on an Olympus AX70 fluorescence microscope and images captured using MacProbe software (version 4.4, Applied Imaging).

Construction of luciferase reporter plasmid containing the 5'-upstream regulatory sequence of mDab2ip gene

To analyze the 5'-upstream regulatory sequence of the *mDab2ip* gene, a 1.3kb fragment from –730 to +545 (transcription initial site as +1 predicted by 5'RACE data) containing upstream region, exon Ia and partial intron 1a was amplified by PCR from clone 22N15. To further define the promoter region in *mDab2ip* gene, a series of deletion mutants were generated by PCR (Table 1). The PCR products were subcloned into pCR^{â}-Blunt II TOPO vector (Invitrogen). After sequencing confirmation, they were further cloned into pGL3 basic vector (Promega) using KpnI/XhoI sites to generate pGL3-F1/R2 (from –730 to +545), pGL3-F6/R2 (form-421 to +545), pGL3-F8/R2 (from +6 to +545), pGL3-F10/R2 (from +249 to +545), pGL3-F12/R2 (from +445 to +545), The pGL3-F7/R2 contains a NcoI fragment (from –147 to +545) of *mDab2ip*. The pGL3-F6/Nco I contains a 0.3 kb insert from –421 to -157 and pGL3-F6/SanD I contains a 0.4 kb insert from-421 to -97.

For Mutagenesis studies, we used pGL3-F7/R2 as template to generate deletion mutants: pGL3-ΔSp1 (deletion of potential Sp1 site from -124 to –114) and pGL3-ΔAP2 (deletion of potential AP2 site from –47 to –26) using Quikchange® II XL Site-Directed Mutagenesis Kit (Stratagene) with the primer set (Table 1).

Measurement of mDab2ip putative promoter activity using reporter gene assay

Both TRAMP-C1 and TRAMP-C3 were plated at a density of 0.6×10^5 cells per well in a 6-well plate. After 16 hrs, cells were transfected with both 0.8 μg of reporter vectors and 0.2 μg β-galactosidase vector (pCH110) using Lipofectamine Plus transfection reagent (Invitrogen). Twenty-four hours after incubation, the transfected cells were treated with TSA for 24 hrs, 5'-Aza for 48 hrs, or combination of both drugs by incubating 5'-Aza for 24 hrs then adding TSA for an additional 24 hrs. Cells were washed twice with cold phosphate-buffered saline (PBS) and harvested them in Lysis Buffer (Promega) then cell lysate was subjected to luciferase and β-galactosidase (β-gal) assays as described previously (Chen *et al.*, 2003). The relative luciferase activity (RLA) from each sample was determined by normalizing the luciferase activity with its β-gal activity. All experiments were repeated at least three times in triplicate.

Chromatin Immunoprecipitation (ChIP) assay

Chromatin Immunoprecipitation (ChIP) assay was performed as described previously (Chen et al. 2003) with a specific PCR primer (Table 1). Precleared chromatin from 2 $x10^6$ cells was used for each ChIP sample. The 5μg anti-Acetyl Histone H3

(Upstate) antibodies used in the per ChIP assays. The immunoprecipitated DNA was amplified by genomic-PCR and the PCR products were subjected gel electrophoresis.

Bisulfite Genomic Sequencing

High molecular weight genomic DNA was obtained from NIH-3T3, TRAMP-C1, TRAMP-C2 and TRAMP-C3 cell lines and subjected to bisulfite modification as previously described (Chen et al. 2003). Bisulfite-modified DNA was amplified by PCR with specific primer set (Table 1). The PCR products were subcloned into the TA cloning vector pCR2.1-TOPO. Five to Seven individual clones were sequenced using reverse M13 primer.

RESULTS

Characterization of mDab2ip gene

A mouse bacterial artificial chromosomal (BAC) library was screened with two partial *mDab2ip* cDNA probes. Three positive clones were identified (22N15, 301E21, and 538A16). Two of them (22N15 and 301E21) were chosen for further study because both contained *mDab2ip* gene confirmed by PCR and Southern blot analysis using a 800-bp partial *mDab2ip* cDNA probe (data not shown). We performed sequencing analysis using Sp6 and T7 primers to analyze both clones. With BLAST program (NCBI, http://www.ncbi.nlm.nih.gov), we matched these two clones with the Mus musculus chromosome 2 genomic contig sequence (accession no. NT_039206). The sequence data showed the 3'end sequencing (T7 primer) of clone 22N15 aligned with the middle portion of the *mDab2ip* gene and the 5' end sequence (Sp6 primer) aligned with 5' upstream of NT_039206. The sequence of clone 301E 21 spans the entire *mDab2ip* gene except 5' upstream regulation region (Fig. 1A). Furthermore, we performed FISH analysis using 22N15 and 301E21 as probes, we were able to locate *mDab2ip* gene at chromosome 2B (Fig. 2A and B).

We deduced the exon-intron junction of *mDab2ip* by aligning its cDNA sequence with NT_039206. Furthermore, we confirmed all predicted exon–intron boundaries by PCR and DNA sequencing, which junction coincides with the GT…AG rule. It appears that *mDab2ip* gene contains 14 exons and 13 introns (Fig. 1A and Tables 2 and 3). Noticeably, exon 1 is a non-coding exon that was separated from exon 2 by a large intron

(>10 kb). The translation initiation site (ATG) is mapped at the 11-bp downstream from the 5'-end of exon 2 and the protein termination site (TAA) is located at exon 14 followed with a large untranslated sequence.

To further determine the transcription starting site(s) of *mDab2ip* gene, we designed two *mDab2ip* specific primers (Sp1, Sp2) to combine with universal outer and inner adapter primers for nested PCR (Fig. 1B). As show in Fig. 1C, two PCR transcripts (300 bp and 600 bp) were detected from RNA isolated from mouse brain and two mouse prostatic epithelial cell lines (TRAMP-C1 and -C2). In contrast, only one single transcript (300 bp) was detected from kidney RNA. DNA sequencing data revealed at least three variants form the exon 1. The *mDab2ip* mRNA from mouse brain and TRAMP-C contains both exon Ia and exon Ib; the *mDab2ip* mRNA from mouse kidney contains exon Ic.

A high homology of deduced protein sequence among mouse Dab2IP, human and rat DAB2IP

In our recent study (Chen *et al.*, 2002), we show that the deduced Dab2IP protein sequence is remarkably similar between rat and human (94% homology). To obtain the entire open reading frame of mDab2IP, we performed RT-PCR from RNA isolated from mouse brain using primer sets based on rat *DAB2IP* cDNA sequence (Chen et al., 2002; Wang et al., 2002). The deduced 1065 amino acids of mDab2IP revealed a high homology sequence with human and rat counterpart (Fig. 3A). Using the program "NCBI conserved domain database " (http://www.ncbi.nih.gov/structure/cdd/wrpsb.cgi),

ScanProsite program (http://au.expasy.org/cgi-bin/scanprosite) and Motif Scan Graphic program (http://scansite.mit.edu), there are five conserved protein domain predicted: PH (pleckstrin homology domain 30-79), C2 (protein kinase C conserved region2 [CalB, amino acid 90-189), RasGAP (GTPase-activating protein, amino acid 212-539), proline-rich domain (amino acid 796-805), and a leucine zipper domain (amino acid 911-932) (Fig. 3B). These data indicate that mDab2IP appear to be a new member of RasGAP family protein.

Expression profile of mDab2ip mRNA in different mouse tissues and cell lines

To determine the tissue distribution of *mDab2ip* mRNA, we performed a real-time RT-PCR analyses (Fig. 4A). Results indicated a unique expression pattern in certain organs. For example, *mDab2ip* was most abundant in brain (72.5-fold), salivary gland (38.7-fold) and testis (21.3-fold); moderate expression in kidney (15.0-fold) and heart (11.3-fold); low expression in lung (7.4-fold), seminal vesicle (7.1-fold), ventral prostate (6.5-fold), epididymis (6.1-fold), liver (5.9-fold) and bladder (5.6-fold); very lower expression in coagulation gland (3.6-fold) and skeleton muscles (2.0-fold) compared with spleen that has the lowest expression level (= 1.0) among all the organs tested. This pattern of expression is consistent with our previous report (Wang et al., 2002) and gene card expression pattern (http://bioinformatics.weizann.ac.il/cards-bin/arddisp?DAB2IP) except the expression level of *Dab2ip* detected from heart.

In several established mouse cell lines, we also observed differential expression level of *mDab2ip* transcript. In general, the highest level of *mDab2ip* mRNA was

detected in NIH 3T3 cell line (≈ 8.5-fold higher than TRAMP-C3); TRAMP-C1 and -C2 line (≈3-fold) had moderate expressions and TRAMP-C3 line had the lowest expression (Fig. 4B). PC-3, a human prostate cancer cell line, was used as a negative control (Chen et al., 2002).

Analysis of the 5'-upstream sequence of the mDab2ip gene

To analyze the promoter region of the *mDab2ip* gene, a 1.3kb fragment from position –730 to +545 (transcription initial site as +1 predicted by 5'RACE) containing 5' upstream region of the exon Ia, exon Ia and partial intron1a region was amplified by PCR from clone 22N15 using primer set F1/R2 (Table 1). Sequencing analysis indicated that this region is very GC-rich. Using TFSEARCH program (http://www.cbrc.jp/research/db/TFSEARCH.html); Promoter Scan II program (http://thr.cit.nih.gov/molbio/proscan/) and MacVector 7.0 program, we identified several potential *trans*-factor binding sites (Fig. 5A) including Sp1, AP-1 AP-2, SREBP, and p300, GATA-1/2, PEA2, AML-1a and MalT_box. Neither TATA-box nor CAAT-box was identified. The similar *trans*-factor binding sites were also detected in *hDAB2IP* gene (Chen *et al*., 2002). It indicates that *Dab2ip* gene is a typical TATA-less promoter.

To define the potential promoter region in the *mDab2ip* gene, we examined the reporter gene activities of a series of deletion constructs (Fig. 5B) generated from the clone 22N15. Consistent with Fig. 4B, the luciferase activity of *mDab2ip* promoter constructs was much higher in NIH-3T3 cell than two other mouse prostatic epithelial cells (Fig. 5C).

Using both TRAMP-C1 and TRAMP-C3 cells (Fig. 5D), we observed both constructs (pGL3-F6/R2 [form -421 to +545] and pGL3-F7/R6 [from -147 to +545]) expressed higher levels of luciferase reporter gene than that of pGL3-F1/R2 (from –730 to +545), suggesting that the presence of a negative *cis*-element between -730 and –421. On the other hand, the reporter gene activity decreased significantly in the rest of deletion constructs (i.e., pGL3- F8/R2, pGL3- F10/R2, pGL3- F12/R2). Also, very little reporter gene activity was observed in cells transfected with either pGL3 F6/NcoI (from -421 to –157) or pGL3-F6/SanDI (from-421 to –97). We therefore conclude that the basal promoter region of *mDab2ip* gene is between -147 and +545. Noticeably, a good correlation between the *mDab2ip* mRNA level and the reporter gene activity was observed in these TRAMP-C cells, indicating that this is a promoter operative in mouse prostatic epithelial cells

However, to further identify the role of *cis*-elements such as Sp1 and AP2 in modulating promoter activity in TRAMP-C1 and TRAMP-C3 cells, we transfected either pGL3-ΔSp1, or pGL3-ΔAP2 into these cells. The luciferase activity of both mutants did not alter in these two cell lines (Fig. 5D). In contrast, the luciferase activities of both mutants in NIH-3T3 cell line reduced dramatically (Fig. 5E), suggesting that Sp1 and AP2 site are critical for *mDab2ip* gene promoter activity in NIH-3T3.

Epigenetic regulation of mDab2ip promoter activity in prostatic epithelium

To understand the underlying mechanism(s) leading to the down regulation of *mDab2ip* gene expression in TRAMP-C3 cells, two common epigenetic regulatory

pathways (ie., histone acetylation and DNA methylation) were analyzed using epigenetic modifiers such as TSA and 5'-Aza. TSA and/or combination were able to induce promoter (pGL3-F6/R2) activity, but slight induce by 5'-Aza (Fig. 5F). A similar induction pattern was detected using the full-length pGL3-F1/R2 promoter (data not shown). We further observed corresponding induction *mDab2ip* mRNA in the TRAMP-C3 cells (Fig. 6A).

To correlate the status of acetyl histone H3 associated with the *mDab2ip* promoter region, a ChIP assay was performed. The elevated levels of acetyl histone H3 were associated with the promoter region (from –154 to +7) in TRAMP-C3 cells treated with TSA or the combination, but slight increase by 5'-Aza (Fig. 6B), indicating that TSA could increase histone acetylation level in *mDab2ip* gene promoter, which is consistent with transcriptional elevated levels of gene activity (Fig. 5F and Fig 6A).

To examine the DNA methylation status of *mDab2ip* promoter in mouse prostatic epithelia, we used a bisulfite DNA sequencing assay to determine the density of methylated CpG islands (from +8 to +294 region). Data from four cell lines (NIH-3T3, TRAMP-C1, TRAMP-C2 and TRAMP-C3) indicated that DNA methylation was rarely detected at the CpG sites (Fig. 6C). Taken together, we believe that histone acetylation play a key role in modulating *mDab2ip* gene expression, but slight effect by DNA methylation

DISCUSSION

The *mDab2ip* gene spans approximately 65kb containing 14 exons and 13 introns with at least three variants: exon Ia, exon Ib and exon Ic found from different sources of RNA using 5'RACE assay. All three splicing sequences of *mDab2ip P* cDNA have been submitted to the GenBank™ (AY305656 [*mDab2ip a*]; AY 305657 [*mDab2ip b*]; AY305658 [*mDab2ip c*]). Using FISH analysis, *mDab2ip* was localized at chromosome band 2B (Fig. 2), which is consistent with the LocusLink program analysis (http://www.ncbi.nih.gov/ LocusLink).

In this study, we performed a real-time RT-PCR to demonstrate the *mDab2ip* mRNA levels in different organs (Fig. 4A). Very abundant *mDab2ip* mRNA levels were found in brain, salivary gland and testis and the moderate levels were found in kidney and heart. In addition, organs such as lung, seminal vesicle, ventral prostate, epididymis, liver and bladder only express low levels of *Dab2ip* mRNA. Also, the lowest level of *Dab2ip* mRNA was detected in coagulation gland, skeletal muscles and spleen. Such diverse expression pattern of *Dab2ip* gene implies that *m Dab2ip* may have a unique physiological function in specific organ. To gain the insight of the mechanisms of *mDab2ip* transcriptional regulation, we isolated ~1.3kb (Fig. 5A) fragment containing 5'-upstream region from exon Ia and we found very rich GC-rich sequences and no canonical TATA boxes in this region. Nevertheless, we have shown that the 5'-flanking region from positions –730/+545 could enhance the reporter gene activity and it contained the basal promoter (-147/+545) and a negative regulatory element (-730/-421) (Fig. 5). We also identified several putative *cis*-elements in this region that could underlie the differential *Dab2ip* gene expression in various organs or cells. We further performed

mutagenesis studies (Fig. 5D and E) and predicted the potential binding sites, Sp1 and AP2 in promoter region.

In our previous publications (Chen et al., 2002; Wang et al., 2002), we found the translation initiation site (ATG) of *DAB2IP* at 63-bp from the 5'-end of exon 3 and predicted a putative open reading frame encoding 967-amino acid for hDAB2IP or 996-amino acid for rat DAB2IP (rDAB2IP). However, the updated sequence data from NCBI (accession no. NP_619723) indicate that an additional ATG site is mapped at 11-bp from the 5'-end of exon 2 that was also detected in *mDab2ip*. Thus, predicted mDab2IP protein encodes 1065-amino acid containing an additional 69-amino acid with a PH domain. PH domain is a short motif that mediates membrane localization and is found in many proteins involved in signal transduction, including GAPs for Ras (Rebecchi et al., 1998; Shaw 1996). The predicted protein sequence alignment between mouse and human DAB2IP is remarkable conserved. Von Bergh (Von Bergh et al., 2004) reported that the *hDAB2IP* is the alias for *AF9Q34*gene (accession no. AY032952) as a novel fusion partner of MLL in AML patient with at (9:11). The juxaposition of MLL intron 9 into exon 2 of AF9Q34 will result in the loss of the exon 2 splicing donor site. Consequently, the *hDAB2IP*/AF9Q34 exon 2 sequences will be spliced out and result in a MLL-exon 9/AF9Q34-exon 3 fusion product. In this case, the AF9Q34-MLL fusion protein does not contain PH domain, implying that the normal function of the AF9Q34 gene may be altered due to the chromosomal translocation.

Sequence analysis of mDab2IP revealed the presence of a highly conserved GRD (GAP related domains), the catalytic unit to stimulate the GTPase activity of Ras proteins, in the N-terminus of mDab2IP. GRD is a characteristic domain in the all

RasGAPs such as human neurofiibromin (NF1), rat SynGAP, p120GAP and human nGAP (Glanzer et al., 2002; Li et al., 1996; Kim et al., 1998; Bernards et al., 1992; Davis et al., 1993; Noto et al., 1998). Homayouni *et al.* suggest that Dab2IP may function as a down stream effector in the Reelin-signaling pathway that influences Ras signaling during brain development (Homayouni et al., 2003). With the cloning of this gene from mouse, studying the role of this gene in brain development as well as prostate carcinogeneis will be further facilitated.

We observed induction of both promoter activity and endogenous *mDab2ip* expression following TSA, or combination treatment in the TRAMP-C3, but slight effect by 5' Aza treatment, which can clarify the epigenetic mechanism for *mDab2ip* gene regulation.

Acknowledgments

We thank Dr. Norman Greenberg (Baylor College of Medicine) for providing TRAMP-C cell lines and Kenneth S. Koeneman (UT Southwestern Medical Center) for reading this manuscript. This work is supported in part by United States Army Grant W81XWH-04-1-0222 and DAMD17-03-2-0033.

REFERENCES

Bernards, A., Haase, V.H., Murthy, A.E., Menon, A., Hannigan, G.E., Gusella, J.F. (1992). Complete human NF1 cDNA sequence: two alternatively spliced mRNAs and absence of expression in a meuroblastoma line. DNA Cell Biol. **11,** 727–734.

Chen, H., Pong, R.C., Wang, Z., Hsieh, J.T. (2002). Differential regulation of the human gene DAB2IP in normal and malignant prostatic epithelia: cloning and characterization. Genomics **79,** 573-581.

Chen, H., Toyooka, S., Gazdar, A. F., Hsieh, J.T. (2003). Epigenetic regulation of a novel tumor suppressor gene (hDAB2IP) in prostate cancer cell lines. J. Biol. Chem. **278**, 3121-3130.

Davis, M. M., Catino, J.J., Satoh, T., Kaziro, Y., Perkins, L.M. (1993). Sequence of the cDNA encoding Ras GTPase-activating protein from rat. Gene **134**, 305–306.

Dote, H., Toyooka, S., Tsukuda, K., Yano, M., Ouchida, M., Doihara, H., Suzuki, M., Chen, H., Hsieh, J.T., Gazdar, A.F., Shimizu, N. (2004). Aberrant promoter methylation in human DAB2 interactive protein (*hDAB2IP*) gene in breast cancer. Clin. Cancer Res. **10,** 2082-2089.

Foster, B.A., Gingrich, J.R., Kwon, E.D., Madias, C., Greenberg, N.M. (1997). Characterization of prostatic epithelial cell lines derived from transgenic adenocarcinoma of the mouse prostate (TRAMP) model. Cancer Res. **57,** 3325-3330.

Fulop, V., Colitti, C.V., Genest, D., Berkowitz, R.S., Yiu, G.K., Ng, S.W., Szepesi, J., Mok, S.C. (1998). DOC-2/hDAB2, a candidate tumor suppressor gene involved in the development of gestational trophoblastic diseases. Oncogene **17,** 419–424.

Glanzer, J.G., Liao, L., Baker, T., McMullen, M.H., Langan, A.S., Crandall, L.Z., Vorce, R.L. (2002). Organization and regulation of the human rasGAP gene. Gene **285,** 149-156.

Gingrich, J.R., Barrios, R.J., Kattan, M.W., Nahm, H.S., Finegold, M.J., Greenberg, N.M. (1997). Androgen-independent prostate cancer progression in the TRAMP model. Cancer Res. **57,** 4687-4691.

Greenberg, N.M., DeMayo, F., Finegold, M.J., Medina, D., Tilley, W.D., Aspinall, J.O., Cunha, G.R., Donjacour, A.A., Matusik, R.J., Rosen, J.M. (1995). Prostate cancer in a transgenic mouse. Proc. Natl. Acad. Sci. **92,** 3439-3443.

Homayouni, R., Magdaleno, S., Keshvara, L., Rice, D. S., Curran, T. (2003). Interaction of Disabled-1 and the GTPase activating protein Dab2IP in mouse brain. Mol. Brain Res. **115,** 121-129.

Jones, P.A., Takai, D. (2001). The Role of DNA Methylation in Mammalian Epigenetics. Science **293,** 1068-1070.

Kim, J.H., Liao, D., Lau, L.F., Huganir, R**.** (1998). SynGAP: a synaptic RasGAP that associates with the PSD-95/SAP90 protein family. Neuron **20,** 683–691.

Li, S., Satoh, H., Watanabe, T., Nakamura, S., Hattori, S. (1996). cDNA cloning and chromosomal mapping of a novel human GAP (GAP1M), a GTPase-activating protein of Ras. Genomics **35,** 625–627.

Noto, S., Maeda, T., Hattori, S., Inazawa, J., Imamura, M., Asaka, M., Hatakeyama, M. (1998). A novel human RasGAP-like gene that maps within the prostate cancer susceptibility locus at chromosome 1q25. FEBS Lett. **441,** 127–131.

Rebecchi, M.J., Scarlata, S. (1998). Pleckstrin homology domains: a common fold with diverse functions. Annu. Rev. Biophys. Biomol. Struct. **27,** 503-528.

Shaw, G. (1996). The pleckstrin homology domain: an intriguing multifunctional protein module. Bioessays **18,** 35-46.

Tseng, C.P., Ely, B.D., Pong, R.C., Wang, Z., Zhou, J., Hsieh, J.T. (1999). The role of DOC-2/DAB2 protein phosphorylation in the inhibition of AP-1 activity. An underlying mechanism of its tumor-suppressive function in prostate cancer. J. Biol. Chem. **274,** 31981-31986.

von Bergh, A.R., Wijers, P.M., Groot, A.J., van Zelderen-Bhola, S., Falkenburg, J.H., Kluin, P.M., Schuuring, E. (2004). Identification of a novel RAS GTPase-activating protein (*RASGAP*) gene at 9q34 as an *MLL* fusion partner in a patient with de novo acute myeloid leukemia. Genes Chromosomes Cancer. **39,** 324-334.

Wang, Z., Tseng, C.P., Pong, R.C., Chen, H., McConnell, J.D., Navone, N., Hsieh, J.T. (2002). The mechanism of growth-inhibitory effect of DOC-2/DAB2 in prostate cancer. Characterization of a novel GTPase-activating protein associated with N-terminal domain of DOC-2/DAB2. J. Biol. Chem. **277,** 12622-12631.

Wolffe, A.P., Matzke, M.A. (1999). Epigenetics: Regulation through repression. Science **286,** 481-486.

Zhang, R., He, X., Liu, W., Lu, M., Hsieh, J.T., Min, W. (2003). AIP1 mediates TNF-α-induced ASK1 activation by facilitating dissociation of ASK1 from its inhibitor 14-3-3. J. Clin. Invest. **111,** 1933-1943.

Zhang, H., Zhang, R., Luo, Y., D'Alessio, A., Pober, J. S., Min, W. (2004). AIP1/DAB2IP, a novel member of the Ras-GAP family, transduces TRAF2-induced ASK1-JNK activation. J. Biol Chem. **279,** 44955-44965.

Zhou, J., Hsieh J.T. (2001). The inhibitory role of DOC-2/DAB2 in growth factor receptor-mediated signal cascade. DOC-2/DAB2-mediated inhibition of ERK phosphorylation via binding to Grb2. J. Biol. Chem. **276,** 27793–27798.

Zhou, J., Scholes, J., Hsieh, J.T. (2003). Characterization of a novel negative regulator (DOC-2/DAB2) of c-Src in normal prostatic epithelium and cancer. J. Biol. Chem. **278,** 6936-6941.

FIGURE LEGENDS

Fig. 1. Structure of *mDab2ip* gene (A) Map of *mDab2ip* gene dispersed over an approximated 65kb. The exon 1 (black box) contains at least three variants (Ia, Ib, Ic), and the relative position of BAC clones is displayed. (B) Schematic display of two specific primers [Sp1 (outer) and Sp2 (inner)], and corresponding two universal primers for 5'RACE. (C) Alternative slicing of *mDab2ip* mRNA detected from brain, TRAMP-C1/TRAMP-C2, and kidney.

Fig. 2. Chromosomal localization of *mDab2ip* gene by FISH analysis (A) A DAPI stained chromosomes (blue) with hybridized probe (red) and (B) a reversed image of the chromosomal staining.

Fig. 3. The predicted functional domain of the *mDab2IP* protein (A) Alignment of mouse (m) Dab2IP, human (h) and rat (r) DAB2IP proteins exhibited a high sequence homology. Potential functional domains are *shaded and underlined*. *Shaded letters* indicated the non-identical amino acids. (B) Schematic representation of mDab2IP protein. PH (peckstrin homology domain, amino acids 30-79); C2 (protein kinase C conserved region 2 domain, amino acids 90-189); RasGAP (Ras GTPase-activator domain, amino acids 212-539); PR (proline-rich domain, amino acids 796-805); and LZ (leucine zipper domain, amino acids 911-932)

Fig. 4. Expression profile of *mDab2ip* transcript in various mouse organs and cell lines Real-time RT-PCR was performed to detect the expression level of *mDab2ip* mRNA from different mouse organs (A) and mouse cell lines (B). Mouse actin was used as an internal control. The fold induction was calculated as described in " Material and Method". To calculate the relative level of each sample, the lowest expression level of *mDab2ip* from Spleen (A), or TRAMP-C3 (B) was considered as 1. Variation of each sample is less than 10%.

Fig. 5. Characterization of *mDab2ip* gene promoters (A) The predicted regulatory sequences of the *mDab2ip* gene. Exon Ia sequence of the *mDab2ip* is *underlined*. The putative *cis*-acting elements are boxed. Primer sequences (*Bold letters*) and restriction endonucleases sites (*Bold letters and underlined*) were used in subsequent cloning for reporter constructs. The transcription start site (TSS) as +1 was predicted by 5' RACE. (B) Schematic representation of *mDab2ip* gene promoter region. A series of reporter gene constructs containing different deletion/mutagenic fragment of *mDab2ip* promoter region, was cloned in pGL3 basic vector as described in "Materials and Methods". (C) Relative luciferase activity in various mouse cell lines. (D) Relative luciferase activity to evaluate the putative binding sites (Sp1 and AP2) in NIH-3T3 cells. (E) Relative Luciferase activity (RLA) of the *mDAB2IP* promoter in TRAMP-C1 and TRAMP-C3. (F) The effect of TSA, 5'-Aza, or combination on the *mDab2ip* promoter activity Bars, SD. Statistically significant (*).

Fig. 6. Epigenetic regulation of *mDab2ip* gene promoter (A) Real-time RT-PCR was performed to detect the expression level of *mDab2ip* mRNA in TRAMP-C3 cells treated by TSA, 5'-Aza, or combination. Statistically significant (*). (B) Increased levels of histone H3 acetylation associated with *mDAB2ip* promoter in TRAMP-C3 cells treated by TSA, or combination, but only slight increase with 5'-Aza. ChIP assay was performed using anti-acetyl histone H3 antibody. The qPCR was performed using the primer sets summarized in Table 1 and the results were visualized with gel staining. (C) Profiling DNA methylation pattern in the *mDab2ip* gene promoter region (from +8 to +294) in several mouse cell lines. The PCR products from each sample were subcloned and each clone (horizontal row) was sequenced. The position of CpG dinucleotide site (vertical tick) was indicated. O, unmethylated CpG; ●, methylated CpG.

A

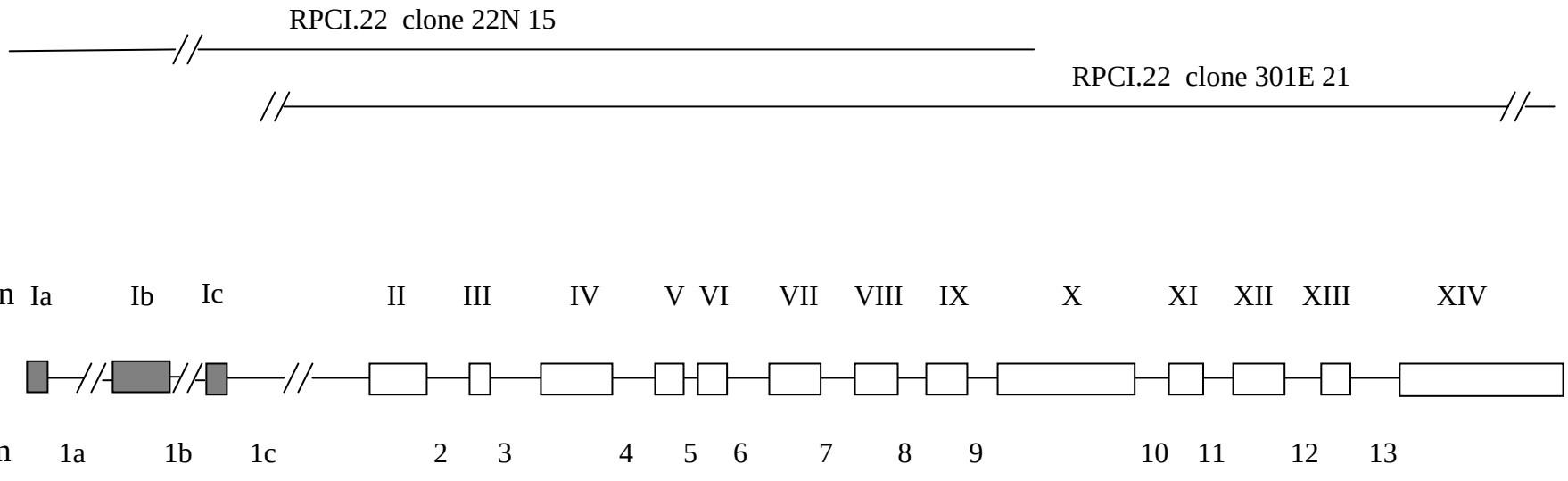
RPCI.22 clone 22N 15
RPCI.22 clone 301E 21
Exon Ia Ib Ic II III IV V VI VII VIII IX X XI XII XIII XIV
Intron 1a 1b 1c 2 3 4 5 6 7 8 9 10 11 12 13

Fig.1

B

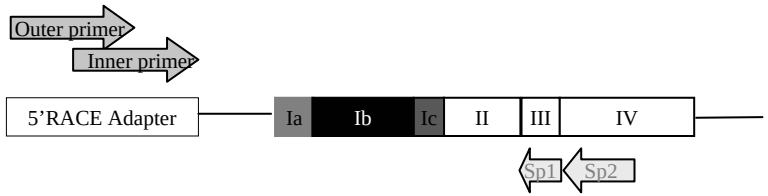
Outer primer
Inner primer
5'RACE Adapter
Ia
Ib
Ic
II
III
IV
Sp1
Sp2

C

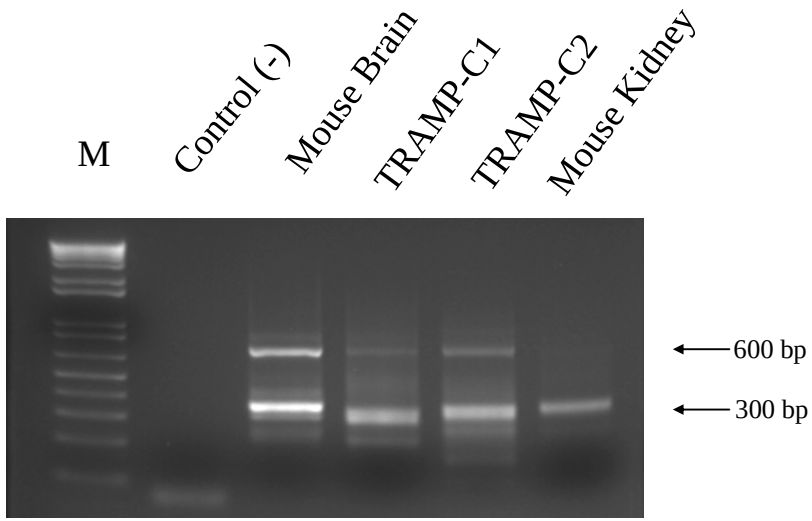
M
Control (-)
Mouse Brain
TRAMP-C1
TRAMP-C2
Mouse Kidney
600 bp
300 bp

Fig. 1

A

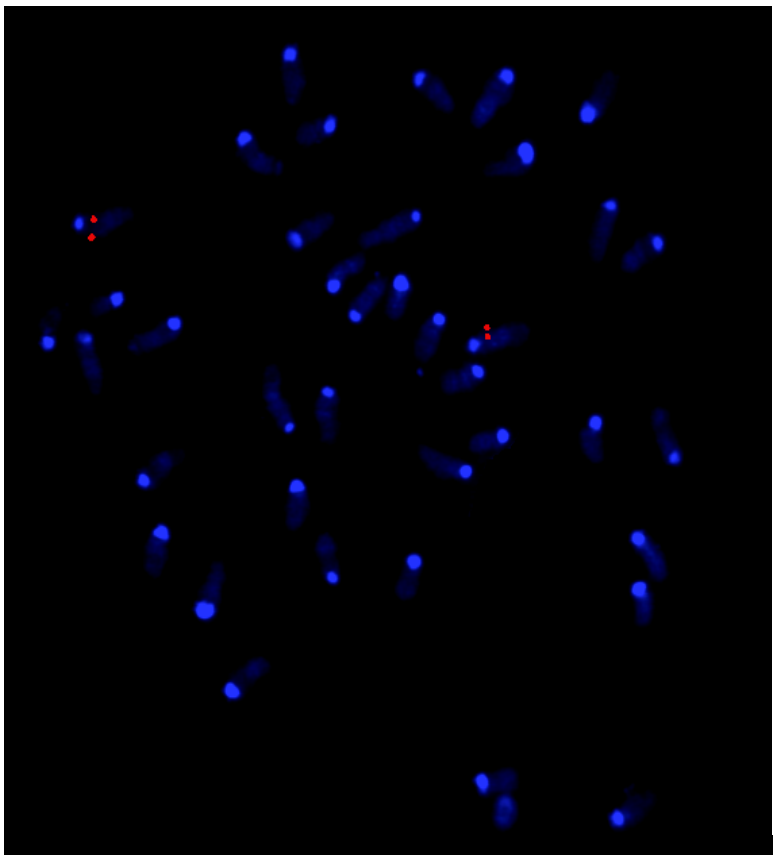

B

Fig. 2

A

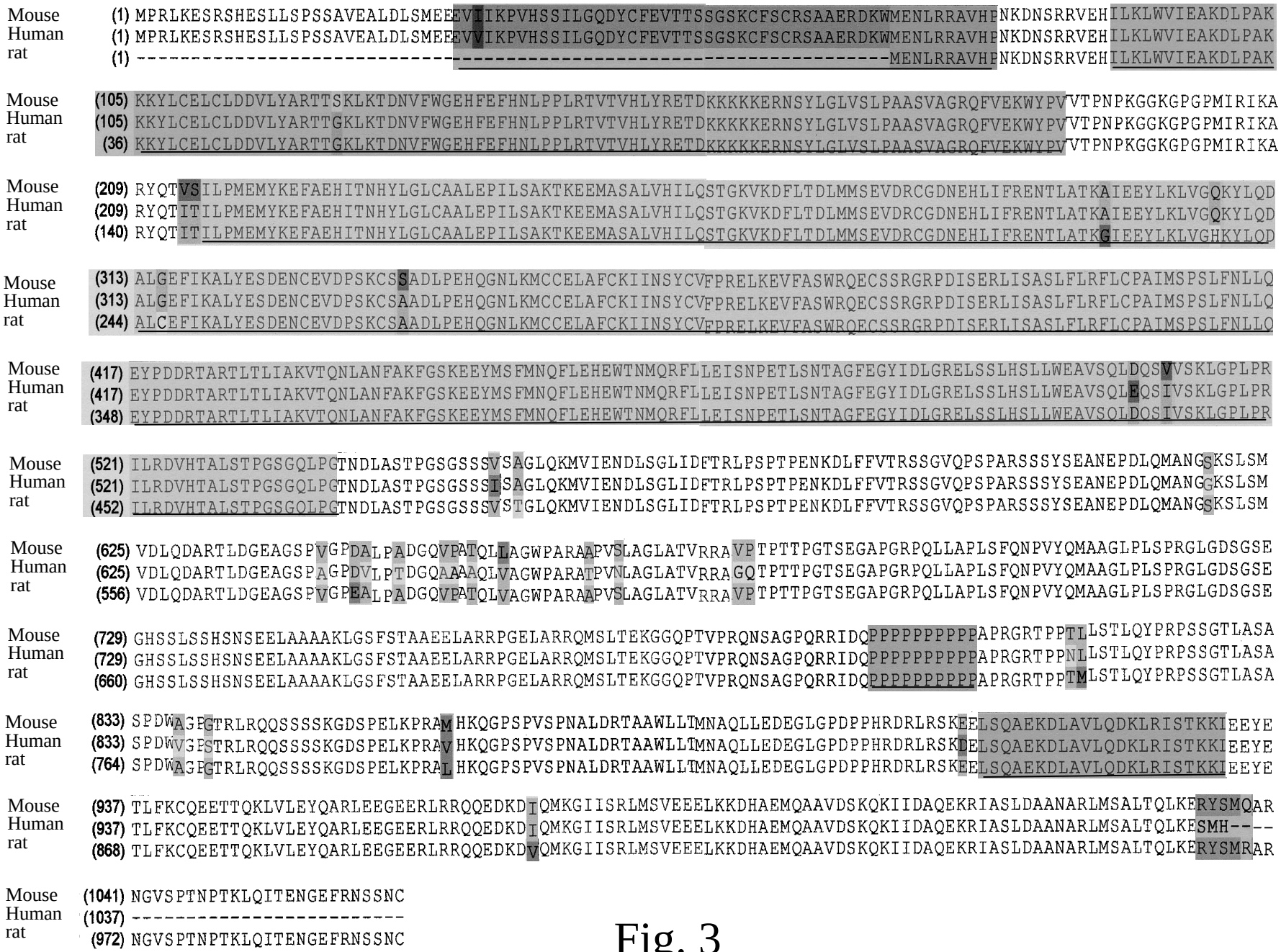
Mouse
Human
rat
(1) MPRLKESRSHESLLSPSSAVEALDLSMEEEVIIKPVHSSILGQDYCFEVTTSSGSKCFSCRSAAERDKWMENLRRAVHPNKDNSRRVEHILKLWVIEAKDLPAK
(1) MPRLKESRSHESLLSPSSAVEALDLSMEEEVVIKPVHSSILGQDYCFEVTTSSGSKCFSCRSAAERDKWMENLRRAVHPNKDNSRRVEHILKLWVIEAKDLPAK
(1) ----------MENLRRAVHPNKDNSRRVEHILKLWVIEAKDLPAK
(105) KKYLCELCLDDVLYARTTSKLKTDNVFWGEHFEFHNLPPLRTVTVHLYRETDKKKKKERNSYLGLVSLPAASVAGRQFVEKWYPVVTPNPKGGKGPGPMIRIKA
(105) KKYLCELCLDDVLYARTTGKLKTDNVFWGEHFEFHNLPPLRTVTVHLYRETDKKKKKERNSYLGLVSLPAASVAGRQFVEKWYPVVTPNPKGGKGPGPMIRIKA
(36) KKYLCELCLDDVLYARTTGKLKTDNVFWGEHFEFHNLPPLRTVTVHLYRETDKKKKKERNSYLGLVSLPAASVAGRQFVEKWYPVVTPNPKGGKGPGPMIRIKA
(209) RYQTVSILPMEMYKEFAEHITNHYLGLCAALEPILSAKTKEEMASALVHILQSTGKVKDFLTDLMMSEVDRCGDNEHLIFRENTLATKAIEEYLKLVGQKYLQD
(209) RYQTITILPMEMYKEFAEHITNHYLGLCAALEPILSAKTKEEMASALVHILQSTGKVKDFLTDLMMSEVDRCGDNEHLIFRENTLATKAIEEYLKLVGQKYLQD
(140) RYQTITILPMEMYKEFAEHITNHYLGLCAALEPILSAKTKEEMASALVHILQSTGKVKDFLTDLMMSEVDRCGDNEHLIFRENTLATKGIEEYLKLVGHKYLQD
(313) ALGEFIKALYESDENCEVDPSKCSSADLPEHQGNLKMCCELAFCKIINSYCVFPRELKEVFASWRQECSSRGRPDISERLISASLFLRFLCPAIMSPSLFNLLQ
(313) ALGEFIKALYESDENCEVDPSKCSAADLPEHQGNLKMCCELAFCKIINSYCVFPRELKEVFASWRQECSSRGRPDISERLISASLFLRFLCPAIMSPSLFNLLQ
(244) ALCEFIKALYESDENCEVDPSKCSAADLPEHQGNLKMCCELAFCKIINSYCVFPRELKEVFASWRQECSSRGRPDISERLISASLFLRFLCPAIMSPSLFNLLQ
(417) EYPDDRTARTLTLIAKVTQNLANFAKFGSKEEYMSFMNQFLEHEWTNMQRFLLEISNPETLSNTAGFEGYIDLGRELSSLHSLLWEAVSQLDQSVVSKLGPLPR
(417) EYPDDRTARTLTLIAKVTQNLANFAKFGSKEEYMSFMNQFLEHEWTNMQRFLLEISNPETLSNTAGFEGYIDLGRELSSLHSLLWEAVSQLEQSIVSKLGPLPR
(348) EYPDDRTARTLTLIAKVTQNLANFAKFGSKEEYMSFMNQFLEHEWTNMQRFLLEISNPETLSNTAGFEGYIDLGRELSSLHSLLWEAVSQLDQSIVSKLGPLPR
(521) ILRDVHTALSTPGSGQLPGTNDLASTPGSGSSSVSAGLQKMVIENDLSGLIDFTRLPSPTPENKDLFFVTRSSGVQPSPARSSSYSEANEPDLQMANGSKSLSM
(521) ILRDVHTALSTPGSGQLPGTNDLASTPGSGSSSISAGLQKMVIENDLSGLIDFTRLPSPTPENKDLFFVTRSSGVQPSPARSSSYSEANEPDLQMANGGKSLSM
(452) ILRDVHTALSTPGSGQLPGTNDLASTPGSGSSSVSTGLQKMVIENDLSGLIDFTRLPSPTPENKDLFFVTRSSGVQPSPARSSSYSEANEPDLQMANGSKSLSM
(625) VDLQDARTLDGEAGSPVGPDALPADGQVPATQLLAGWPARAAPVSLAGLATVRRAVPTPTTPGTSEGAPGRPQLLAPLSFQNPVYQMAAGLPLSPRGLGDSGSE
(625) VDLQDARTLDGEAGSPAGPDVLPTDGQAAAAQLVAGWPARATPVNLAGLATVRRAGQTPTTPGTSEGAPGRPQLLAPLSFQNPVYQMAAGLPLSPRGLGDSGSE
(556) VDLQDARTLDGEAGSPVGPEALPADGQVPATQLVAGWPARAAPVSLAGLATVRRAVPTPTTPGTSEGAPGRPQLLAPLSFQNPVYQMAAGLPLSPRGLGDSGSE
(729) GHSSLSSHSNSEELAAAAKLGSFSTAAEELARRPGELARRQMSLTEKGGQPTVPRQNSAGPQRRIDQPPPPPPPPPPAPRGRTPPTLLSTLQYPRPSSGTLASA
(729) GHSSLSSHSNSEELAAAAKLGSFSTAAEELARRPGELARRQMSLTEKGGQPTVPRQNSAGPQRRIDQPPPPPPPPPPAPRGRTPPNLLSTLQYPRPSSGTLASA
(660) GHSSLSSHSNSEELAAAAKLGSFSTAAEELARRPGELARRQMSLTEKGGQPTVPRQNSAGPQRRIDQPPPPPPPPPPAPRGRTPPTMLSTLQYPRPSSGTLASA
(833) SPDWAGPGTRLRQQSSSSKGDSPELKPRAMHKQGPSPVSPNALDRTAAWLLTMNAQLLEDEGLGPDPPHRDRLRSKEELSQAEKDLAVLQDKLRISTKKIEEYE
(833) SPDWVGPSTRLRQQSSSSKGDSPELKPRAVHKQGPSPVSPNALDRTAAWLLTMNAQLLEDEGLGPDPPHRDRLRSKDELSQAEKDLAVLQDKLRISTKKIEEYE
(764) SPDWAGPGTRLRQQSSSSKGDSPELKPRALHKQGPSPVSPNALDRTAAWLLTMNAQLLEDEGLGPDPPHRDRLRSKEELSQAEKDLAVLQDKLRISTKKIEEYE
(937) TLFKCQEETTQKLVLEYQARLEEGEERLRRQQEDKDIQMKGIISRLMSVEEELKKDHAEMQAAVDSKQKIIDAQEKRIASLDAANARLMSALTQLKERYSMQAR
(937) TLFKCQEETTQKLVLEYQARLEEGEERLRRQQEDKDIQMKGIISRLMSVEEELKKDHAEMQAAVDSKQKIIDAQEKRIASLDAANARLMSALTQLKESMH----
(868) TLFKCQEETTQKLVLEYQARLEEGEERLRRQQEDKDVQMKGIISRLMSVEEELKKDHAEMQAAVDSKQKIIDAQEKRIASLDAANARLMSALTQLKERYSMRAR
(1041) NGVSPTNPTKLQITENGEFRNSSNC
(1037) ----------
(972) NGVSPTNPTKLQITENGEFRNSSNC

Fig. 3

B

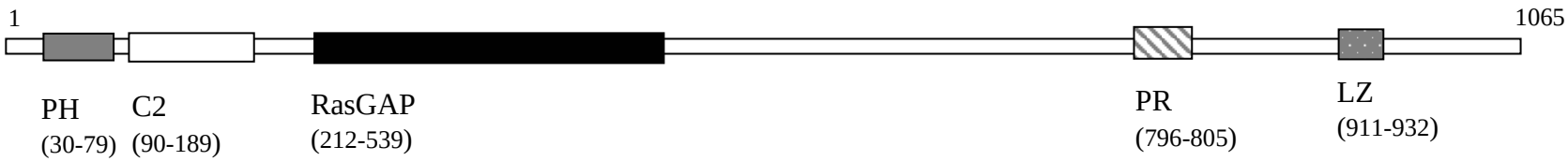

Fig.3

A

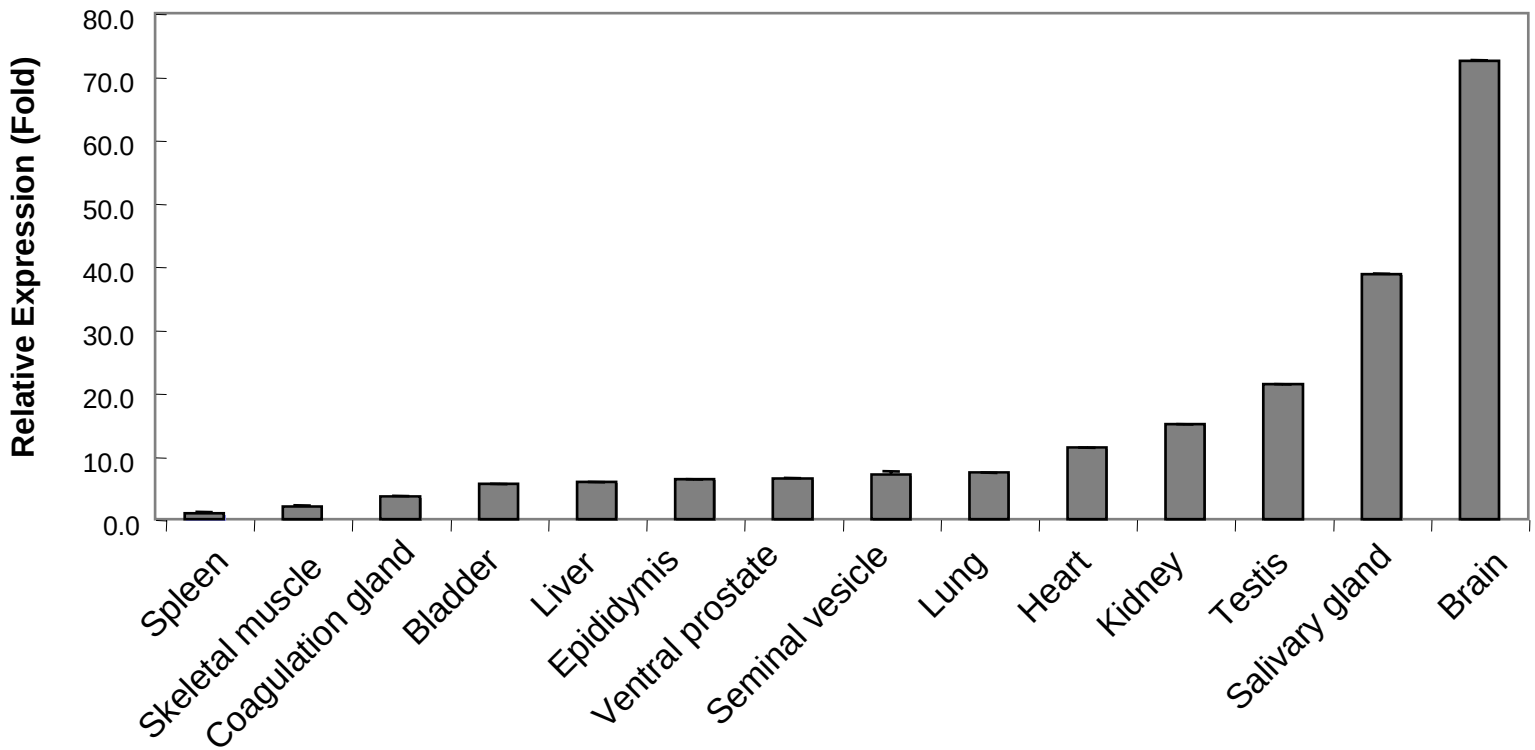
Relative Expression (Fold)
80.0
70.0
60.0
50.0
40.0
30.0
20.0
10.0
0.0
Spleen
Skeletal muscle
Coagulation gland
Bladder
Liver
Epididymis
Ventral prostate
Seminal vesicle
Lung
Heart
Kidney
Testis
Salivary gland
Brain

Fig. 4

B

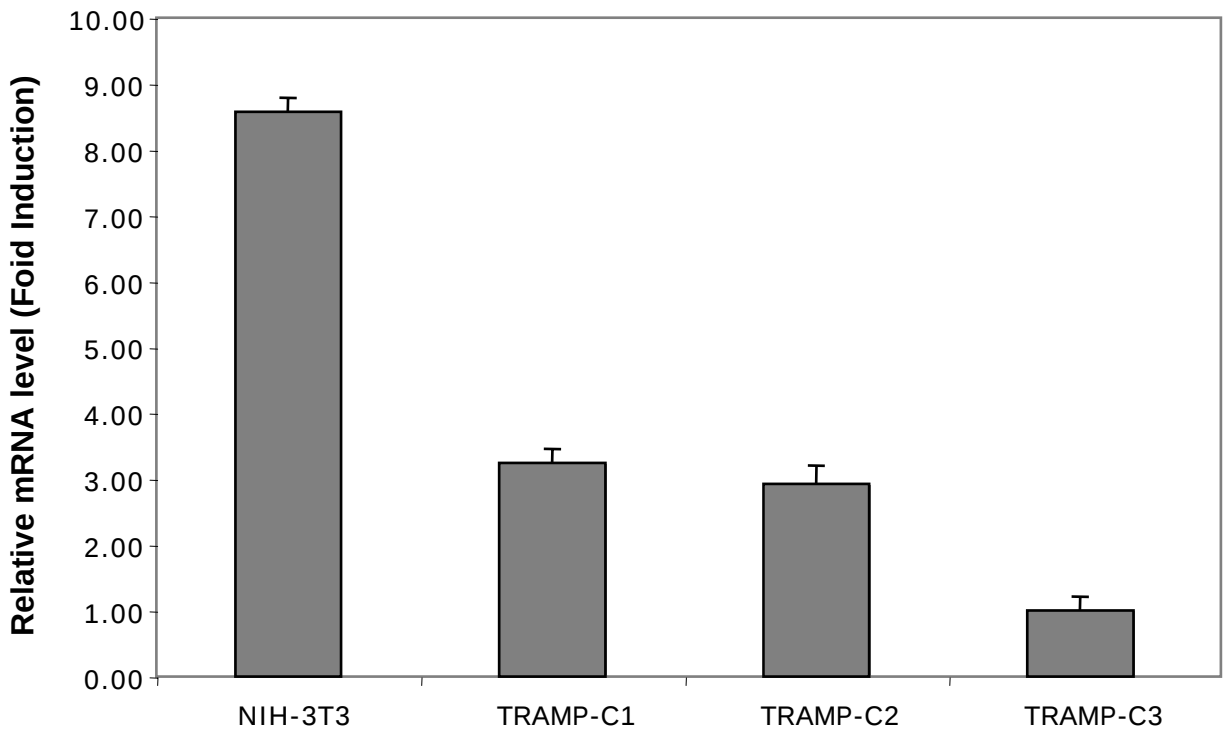
Relative mRNA level (Foid Induction)
10.00
9.00
8.00
7.00
6.00
5.00
4.00
3.00
2.00
1.00
0.00
NIH-3T3
TRAMP-C1
TRAMP-C2
TRAMP-C3

Fig. 4

A


-730
GCTCCTCACCTGCCTCTTCATTAGTCCAGAAGCTCTGACTGGGGTGAGGTGGTGAGCTGGGAATGGCTGGTGAATCCATGCATGATCTGAGACAGGTGTC -630
F1
SREBP
CCCAAATTGGGGACACTCAGCAAACCCTTCAACACCTTGGGCCCCTCCTTAAGGGGTCACTAGAGGATCCTGTACCTATGGGGATTGTTTTTTTTGGGGG -530
GGGGGATCCAAGCGTTTCAGCCTCCATCCTGACATCCAGCCATTGCCTGTCCGCCTTAGGGGGTCTAGATGGCCAGAGTGCTAGTAGGCGCGCTGGCCGT -430
AP-2
MalT_box
GCF
TTGGAGGACCTGCTCTCCCAGCCTTAGTTTCTTTCCTTCATCTTGAGTAACCGCTCCTGTCAGTCCCCCCGACGGGGCGGGGTGTGAGGAATCCTCCTGGA -330
F6
AP-1
Sp1
GGTTGGGGGGTGTGGCCTGGTTGCAGAGGAAGGTGAGGTGAGGGGCTGTTGGTGGCGCAAGCCACTCAACCCGCCCCCACCCCCCAGCCTTGCCGCCCTT -230
Sp1
CCCTCTCAGCGCCGGGGGGCGGAGGGGGGGGCTCGGGCATCCTCGGCCACGGTCGGAGGCACTCGGCTCTGTCGCCATGGCAACGGCGGCTTAGGGGCGGG -130
AP-2
NcoI
GGCGACGTGGCGGGCTGGGCCGCGAGGGTGCGGGTCCCGGCCCGCCGCCGCCGCGCTAACCCCGCCTCCCCTTCCCCCTCTTGTCCGCCCCGCGCCCAGGG -30
Sp1
+1
SanDI
AP-2
CTTCCTCAGCCGCCGCCTCAAGGGCTCCATCAAGCGCACCAAGAGCCAGCCCAAACTGGACCGCAACCACAGCTTCCGCCACATCCTGCCGGGGTTCCGG +70
F8
PEA2
AML-1a
AGCGCAGCCGCCGCCGCCGCGGACAATGAGAGGTGAGCCCGTCGCCGCCCCGGCTGCGCCCCGAGGGCGCGGGGACAAAGCCGGAGCCGGGCAGGGCACT +170
Sp1
TCTCCCGCGGGAGTGACGCCTCGCCAGCCTCCGGGAACTCCGGGAACGGGGCCCCCGTCGTGCTGGGGGACCGGGACTGTACCCTTCGTTGCTTTCACCGG +270
p300
F10
CGCACCTAGGAGGGTGCTGGAGGTCCGGGGTGAGGCCGGGCAGCAAGTGCCCTCTCGGGCATGTGGGGTCCTGCCTCGCCTGGCCGAGGTGGGCATTGTT +370
TTCTGAGCAGTGCTGTGCCTAGAGGTAGGGACGGAAGTGGTGCCTCCACCCTCAGGACCCATCCCCGGGCCTACCGAGTCCCTCGCTGTCCGATACAAAAG +470
GATA-1/2
F12
GCATTTTCGGCTGGTTTTTGCCCAGACCCGGCAGCGCTCGTGGCGTGGAAAAGGGTGAACATCTGGAGGGGAGGAGCA +570
R2
+545

Fig.5

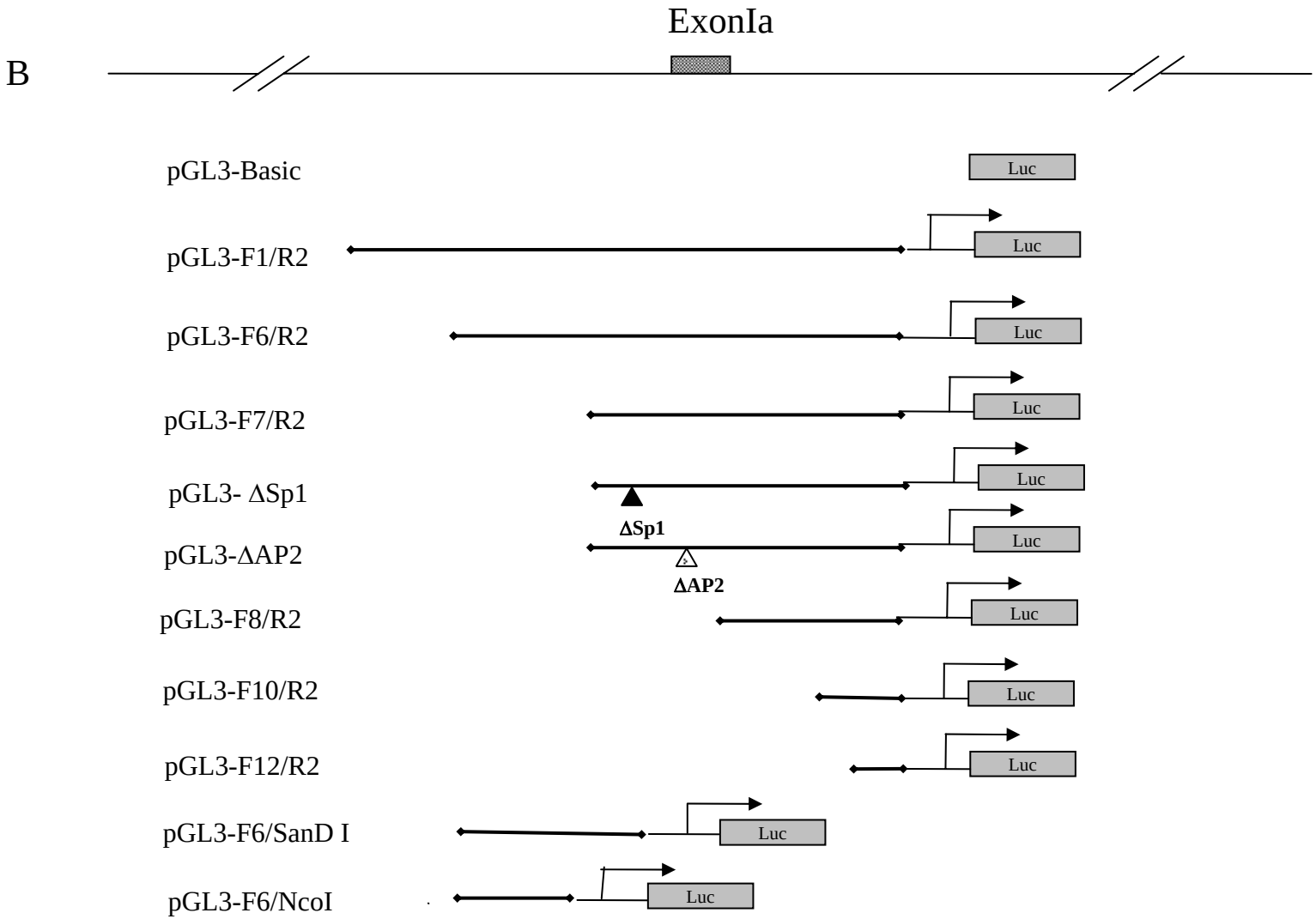
B
ExonIa
pGL3-Basic
Luc
pGL3-F1/R2
Luc
pGL3-F6/R2
Luc
pGL3-F7/R2
Luc
pGL3- ΔSp1
Luc
ΔSp1
pGL3-ΔAP2
Luc
ΔAP2
pGL3-F8/R2
Luc
pGL3-F10/R2
Luc
pGL3-F12/R2
Luc
pGL3-F6/SanD I
Luc
pGL3-F6/NcoI
Luc

Fig. 5

C

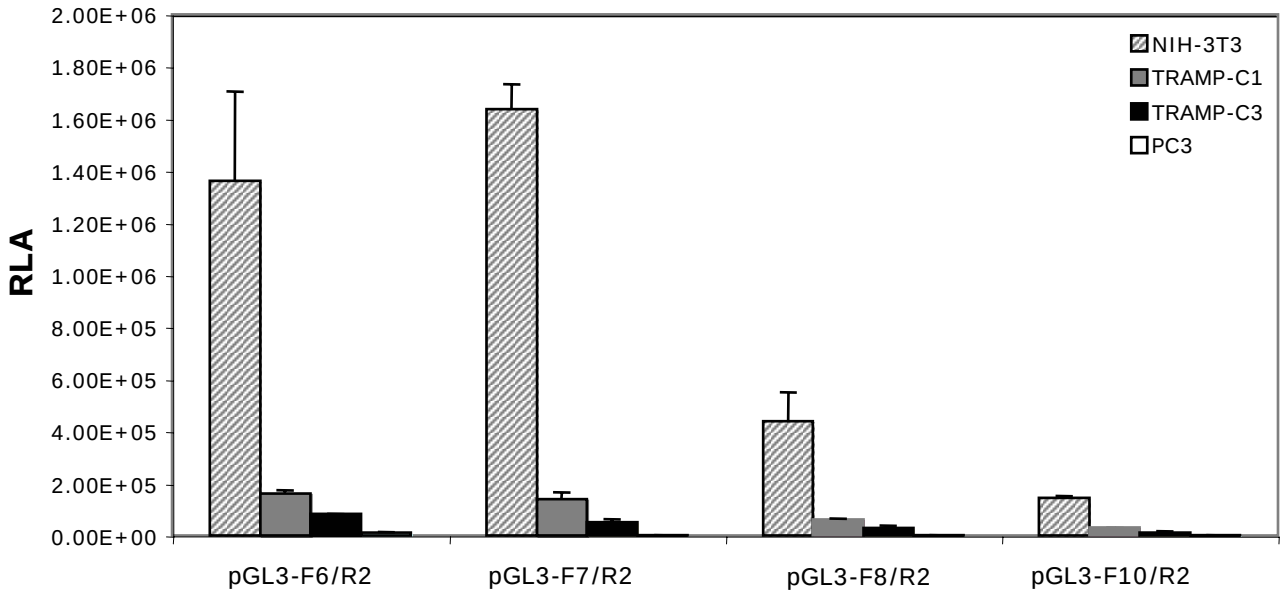
2.00E+06
1.80E+06
1.60E+06
1.40E+06
1.20E+06
1.00E+06
8.00E+05
6.00E+05
4.00E+05
2.00E+05
0.00E+00
RLA
NIH-3T3
TRAMP-C1
TRAMP-C3
PC3
pGL3-F6/R2
pGL3-F7/R2
pGL3-F8/R2
pGL3-F10/R2

Fig.5

D

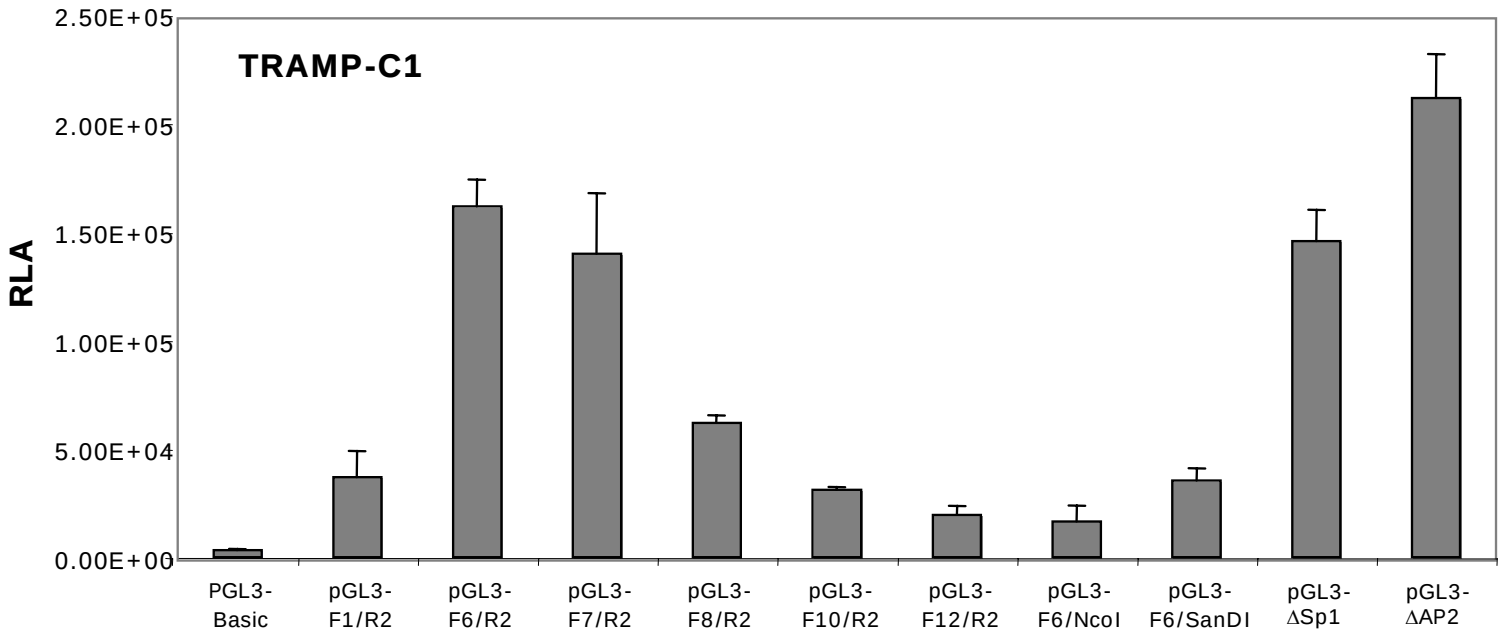
TRAMP-C1
RLA
2.50E+05
2.00E+05
1.50E+05
1.00E+05
5.00E+04
0.00E+00
PGL3-Basic
pGL3-F1/R2
pGL3-F6/R2
pGL3-F7/R2
pGL3-F8/R2
pGL3-F10/R2
pGL3-F12/R2
pGL3-F6/NcoI
pGL3-F6/SanDI
pGL3-ΔSp1
pGL3-ΔAP2

Fig.5

D

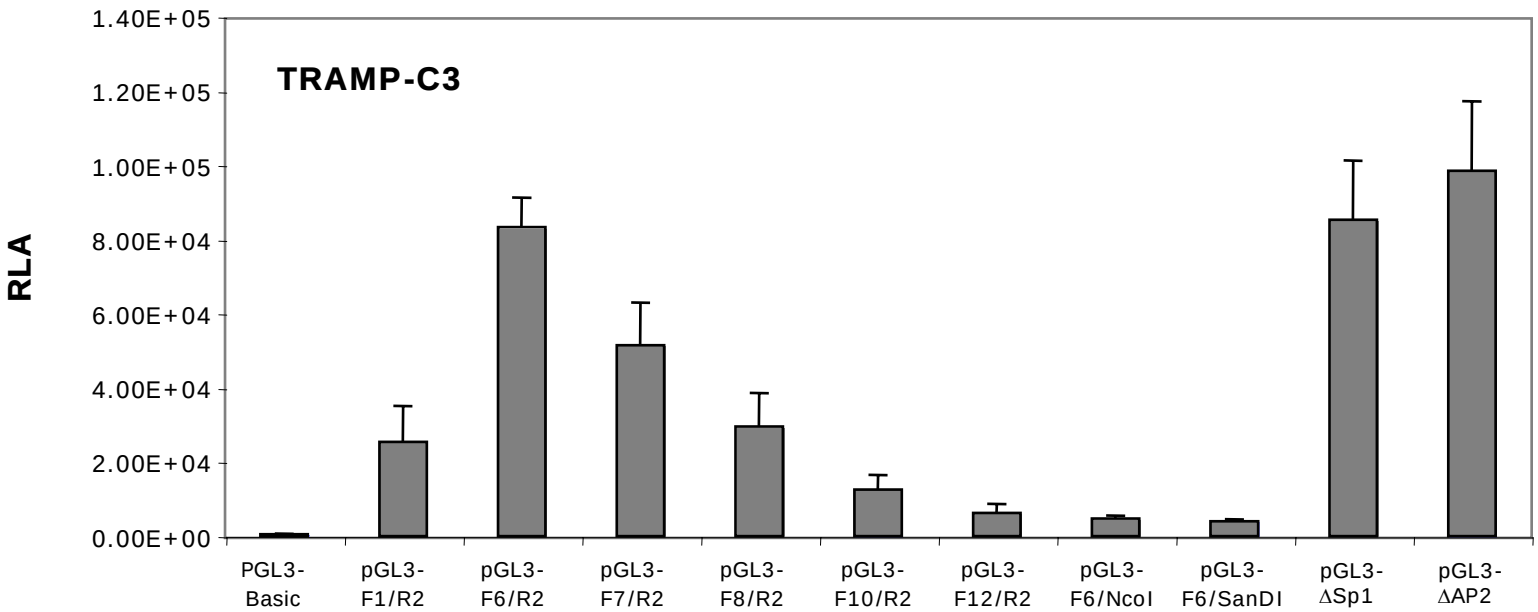
TRAMP-C3
RLA
1.40E+05
1.20E+05
1.00E+05
8.00E+04
6.00E+04
4.00E+04
2.00E+04
0.00E+00
PGL3-Basic
pGL3-F1/R2
pGL3-F6/R2
pGL3-F7/R2
pGL3-F8/R2
pGL3-F10/R2
pGL3-F12/R2
pGL3-F6/NcoI
pGL3-F6/SanDI
pGL3-ΔSp1
pGL3-ΔAP2

Fig.5

E

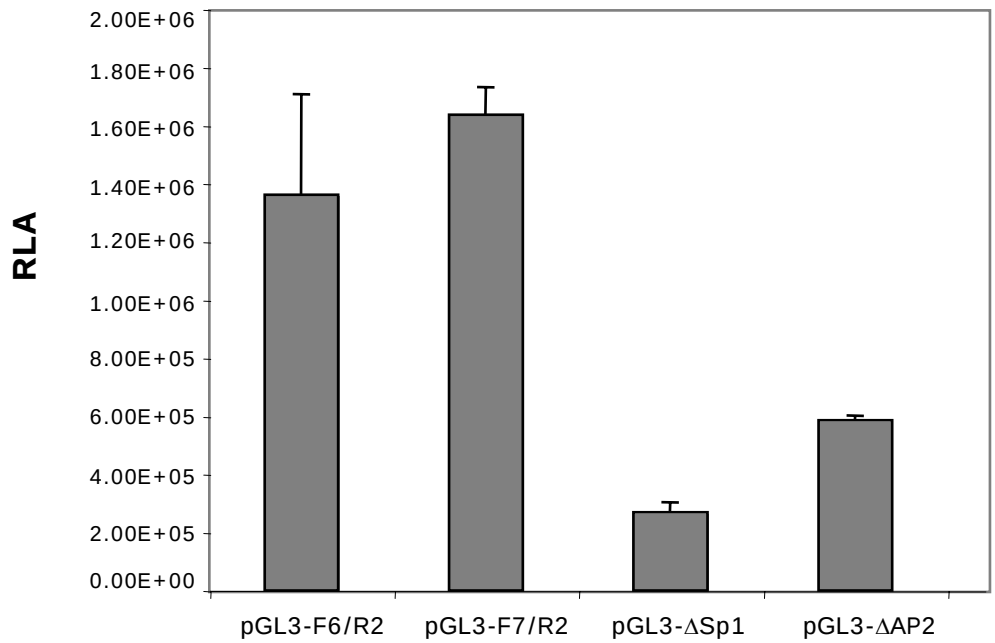
RLA
2.00E+06
1.80E+06
1.60E+06
1.40E+06
1.20E+06
1.00E+06
8.00E+05
6.00E+05
4.00E+05
2.00E+05
0.00E+00
pGL3-F6/R2
pGL3-F7/R2
pGL3-ΔSp1
pGL3-ΔAP2

Fig.5

A

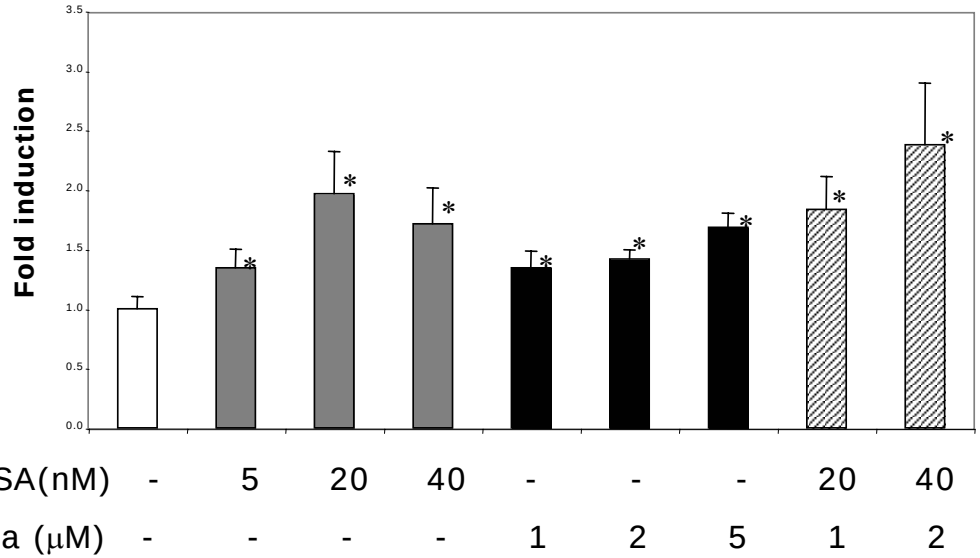
Fold induction
3.5
3.0
2.5
2.0
1.5
1.0
0.5
0.0
TSA(nM) - 5 20 40 - - - 20 40
5'-Aza (μM) - - - - 1 2 5 1 2

B

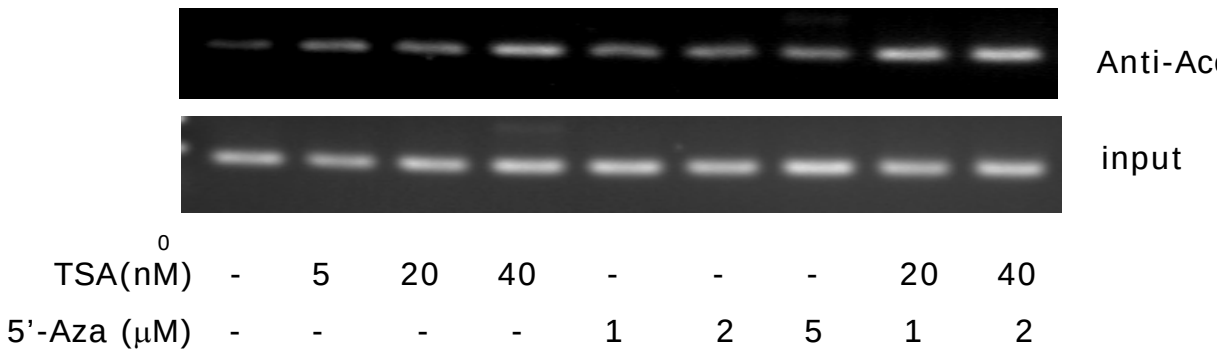
Anti-Acety H3
input
0
TSA(nM) - 5 20 40 - - - 20 40
5'-Aza (μM) - - - - 1 2 5 1 2

Fig.6

C

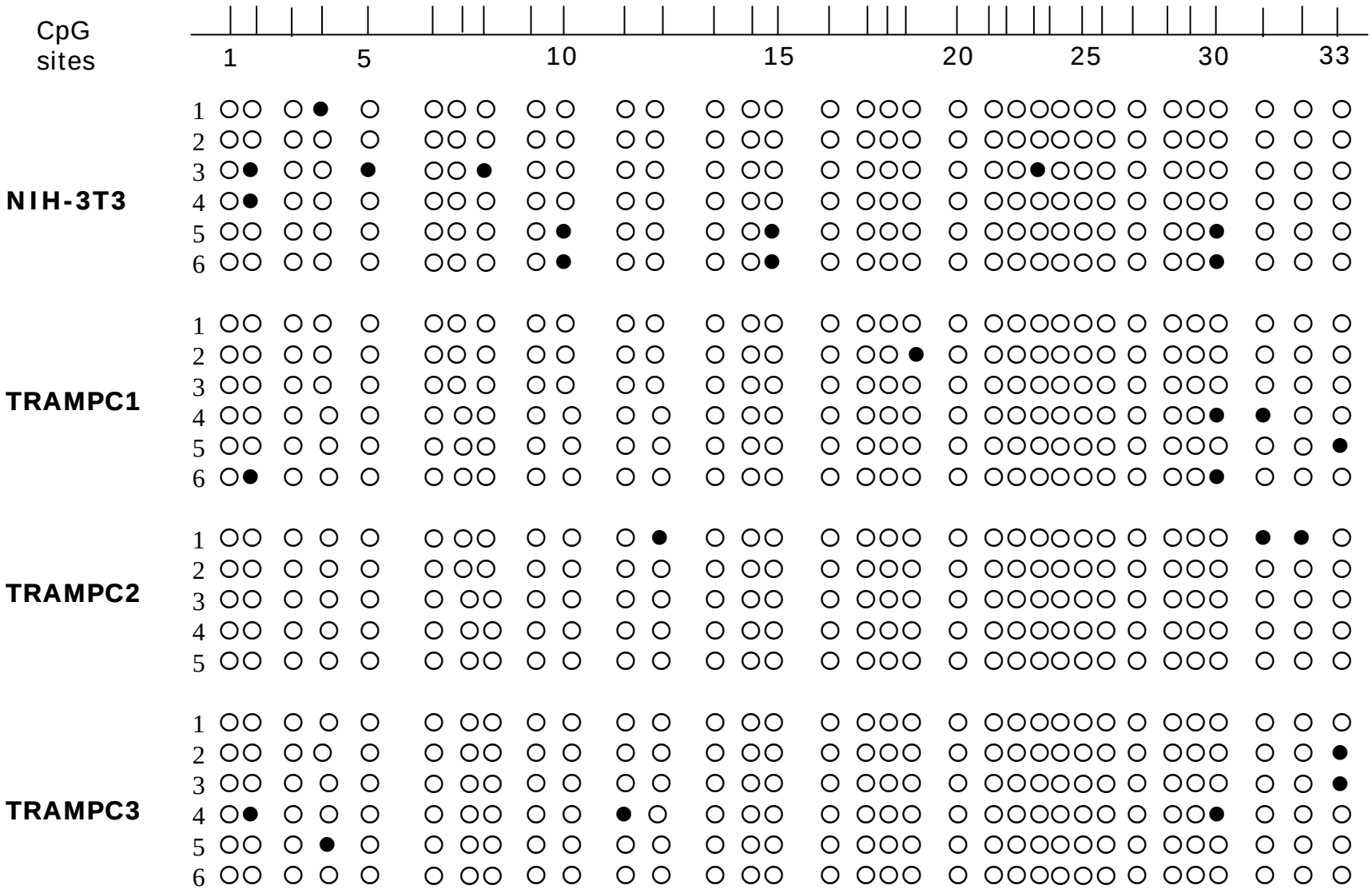

Fig.6